Electronic Supplementary Material (ESI) for Dalton Transactions.

Supporting Information

Synthesis, Structures and Catalytic Behavior of Some BINOL Based Boronates and Boronium Salts

Shipra Garg, Daniel K. Unruh, Clemens Krempner*

Clemens.krempner@ttu.edu

1. General Remarks

All air- and moisture-sensitive manipulations were carried out using standard vacuum line, Schlenk or cannula techniques or in a Vacuum Atmospheres OMNI inert atmosphere dry box containing an atmosphere of purified nitrogen. Triethylphosphine oxide (Alfa Aesar), $(pyrr)_3P{=}NBu^t$ (Aldrich), anhydrous pyridine (Chem-Impex), *rac*-BINOL (Aldrich, 98%) (*R*)-BINOL (Oakwood, 94%) and (*S*)-BINOL (Oakwood, 94%), *rac*-styrene oxide (Aldrich), (*R*)- and (*S*)-styrene oxide (Oakwood) and anhydrous DMSO (Millipore) were purchased from chemical vendors. THF, Ether, toluene and hexanes were distilled under nitrogen from alkali metals and stored over 4 Å molecular sieves. All deuterated solvents were purchased from Cambridge Isotope Labs. THF-D_8, C_6D_6, CD_2Cl_2, $CDCl_3$ and $(CD_3)_2SO$ were dried and stored over 4 Å molecular sieves prior to use. $C_6F_5BH_2{\bullet}SMe_2$ [1] and PhCH=N(O)Me [2] were prepared according to the literature procedures. The NMR spectra were obtained from a JOEL ECS 400 and Varian 500. All measurements, unless noted otherwise, were carried out at 298 K and NMR chemical shifts were given in ppm. The ^{11}B NMR spectra referenced to H_3BO_3 in D_2O (δ = 36 ppm), the ^{31}P NMR referenced to H_3PO_4 in D_2O (δ = 0 ppm), ^{19}F NMR spectrum was referenced to $C_6H_5CF_3$ in C_6D_6 (δ = 62.3 ppm). The ^1H and ^{13}C NMR spectra were referenced to the deuterated solvent peaks. The following abbreviations were used to describe peak multiplicities in the reported NMR spectroscopic data: “s” for singlet, “d” for doublet, “t” for triplet, “q” for quartet, “m” for multiplet and “br” for broadened resonances. Elemental analyses were performed using a Perkin Elmer 2400 Series II CHNS/O Analyzer.

2. Synthetic Procedures

2.1. Synthesis of (*R*)-**1**

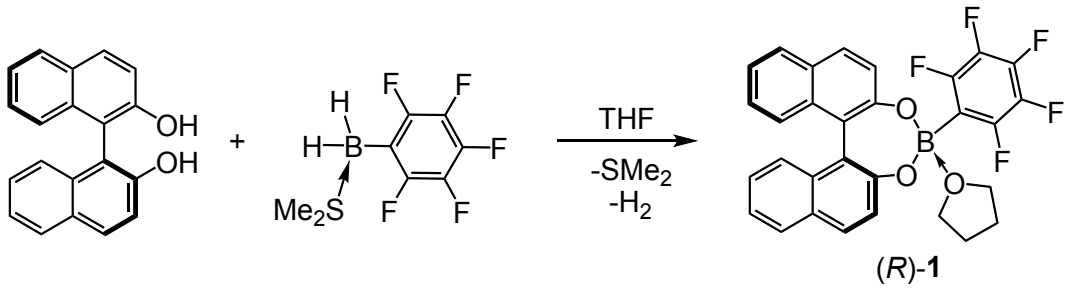

(*R*)-**1**

In the glove box, a 50 ml Schlenk flask was charged with (*R*)-BINOL (354 mg, 1.24 mmol) and 15 mL of dry THF. To this clear solution, a solution of $C_6F_5BH_2$•SMe_2 (315 mg, 1.30 mmol) in THF (10 mL) was slowly added and left for crystallization overnight at room temperature. The obtained crystals were washed twice with THF and subsequently dried under vacuum to give 0.50 g (76%) of (*R*)-**1**. ^{1}H NMR (THF-D_8, 400 MHz): δ 1.67 (CH_2), 3.54 (CH_2), 7.06-7.10 (m, CH arom., 2 H), 7.18-7.27 (m, CH arom., 6 H), 7.76-7.78 (m, CH arom., 4 H) ppm. ^{13}C{H} NMR (THF-D_8, 125.79 MHz): δ 26.7, 68.5, 123.1, 123.5, 124.6, 126.3, 128.0, 129.1, 130.2, 131.7,134.5, 138.4, 141.9, 150.3, 154.6 ppm. ^{19}F NMR (THF-D_8, 376.3 MHz): δ -167.4, -160.4, -134.6 ppm. ^{11}B NMR (THF-D_8, 128.4 MHz): 8.8 ppm. Anal. Calc. for $C_{30}H_{20}BF_5O_3$ (534.29): C, 67.44; H, 3.77; Found C, 66.30; H, 3.58.

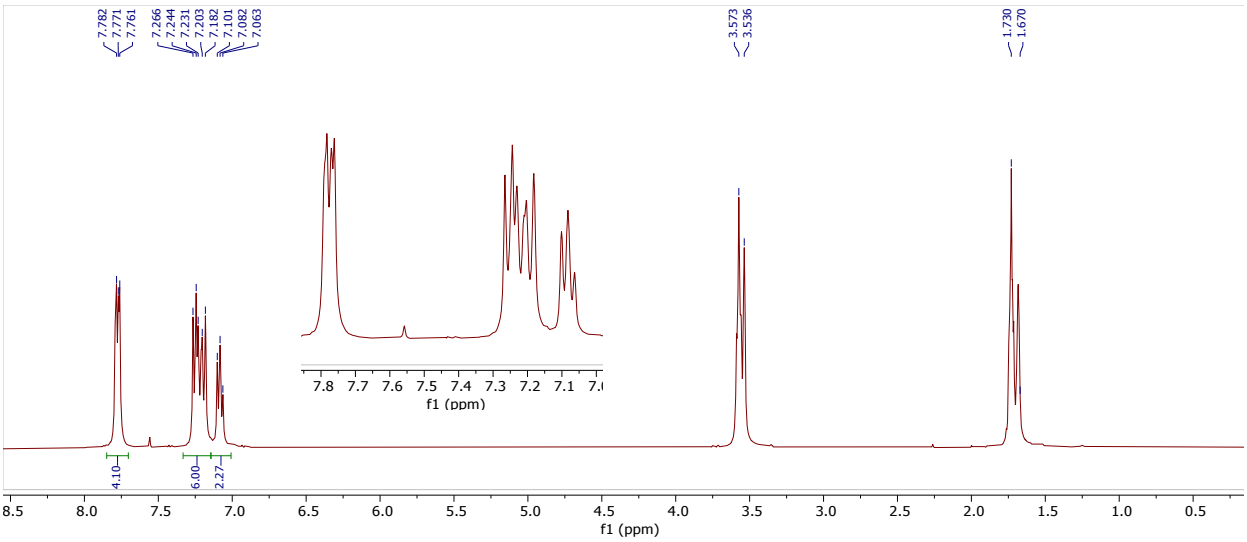

Figure S1. ^{1}H NMR spectrum of (*R*)-**1** in THF-D_8.

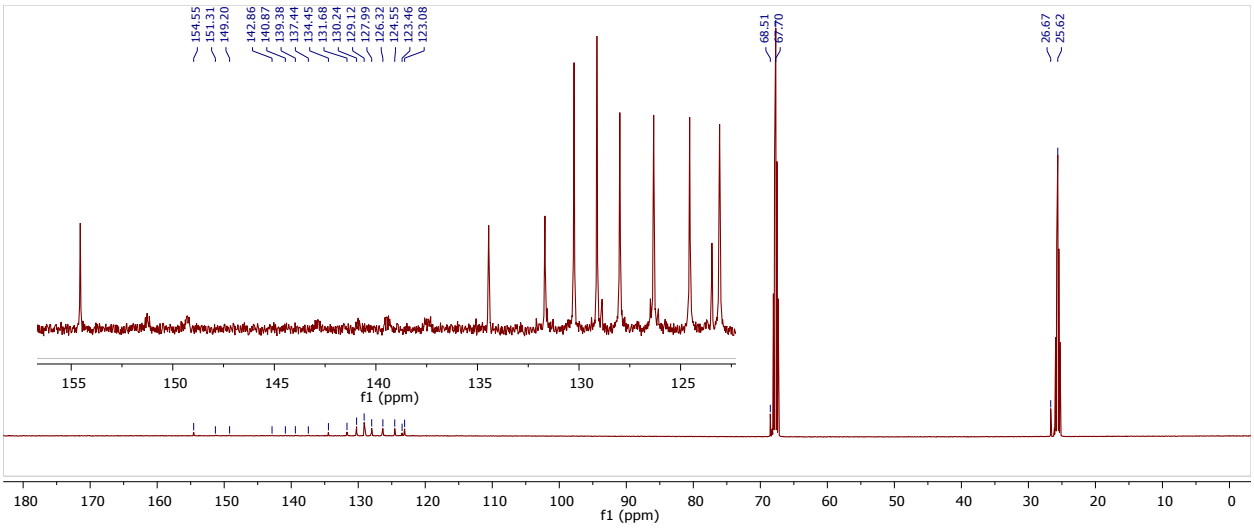

Figure S2. ^{13}C{H} NMR spectrum of (*R*)-**1** in THF-D_8.

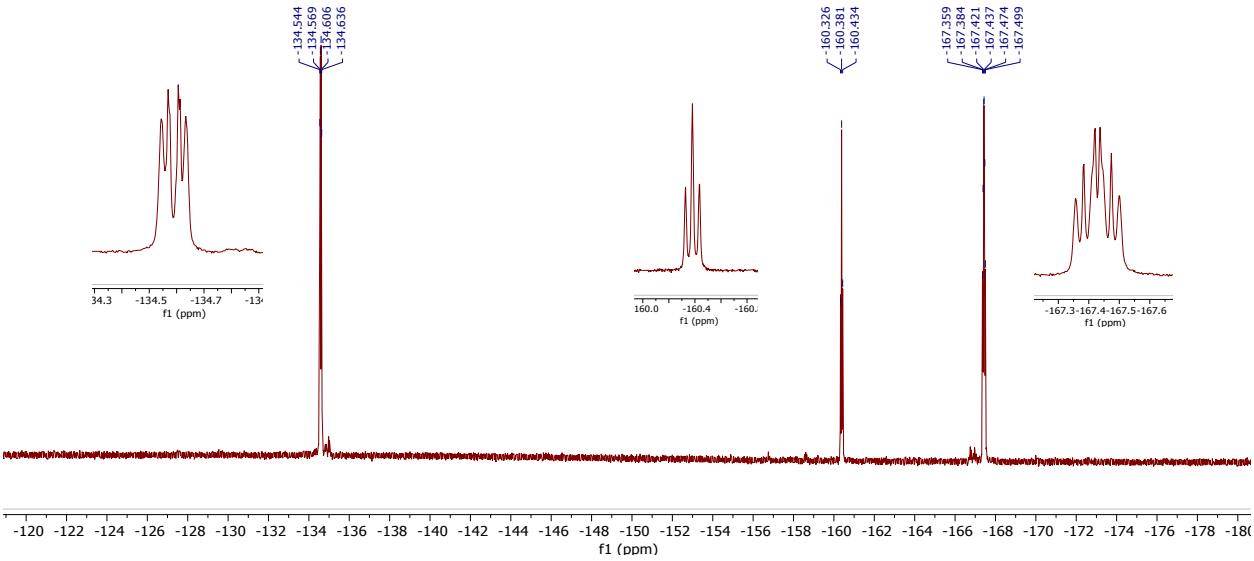

Figure S3. ^{19}F NMR spectrum of (*R*)-**1** in THF-D_8.

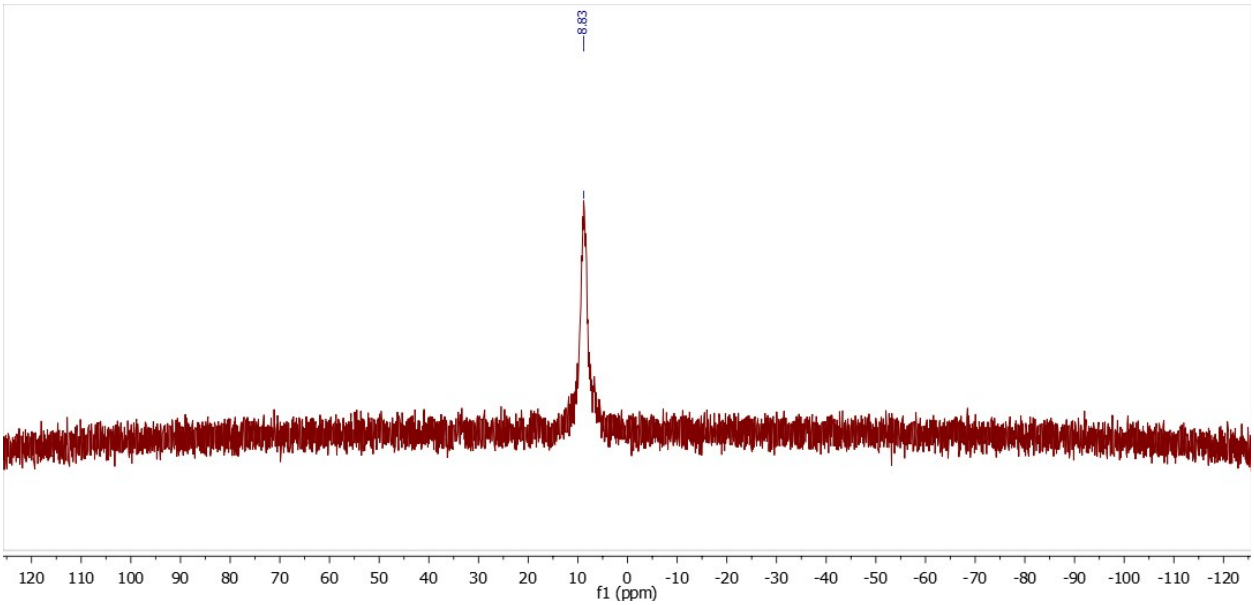

Figure S4. $^{11}B\{H\}$ NMR spectrum of (*R*)-**1** in THF-D_8.

2.2. Synthesis of (*R,R*)-**2**

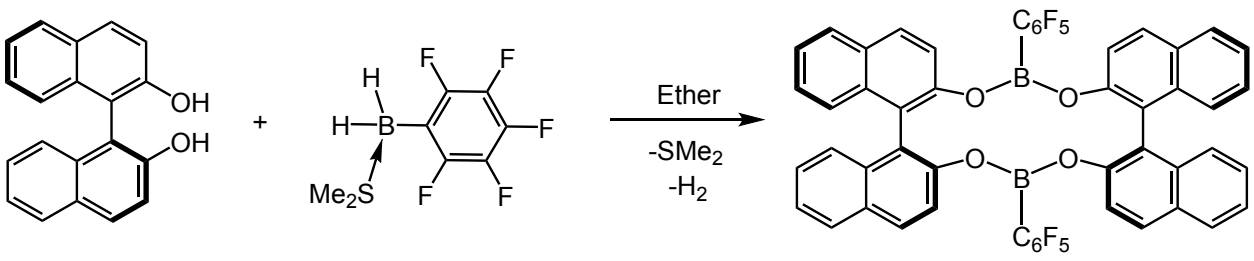

(*R,R*)-**2**

In the glove box, a 50 ml Schlenk flask was charged with (*R*)-BINOL (247 mg, 0.86 mmol) and 15 mL of dry ether. To this clear solution, a solution of $C_6F_5BH_2$•SMe_2 (220 mg, 0.91 mmol) in ether (10 mL) was slowly added and left for crystallization overnight at room temperature. The obtained crystals were washed twice with ether and dried under vacuum to give 255 mg (64%) of (*R,R*)-**2**. ^{1}H NMR (C_6D_6, 400 MHz): δ 6.49 (d, $^3J_{H-H}$ = 9.2 Hz, CH arom., 1 H), 6.90 (t, $^3J_{H-H}$ = 8.4 Hz, CH arom., 2 H), 7.12-7.15 (m, CH arom., 6 H), 7.24 (d, $^3J_{H-H}$ = 7 Hz, CH arom., 1 H), 7.35 (d, $^3J_{H-H}$ = 8.8 Hz, CH arom., 3 H), 7.41(d, $^3J_{H-H}$ = 8.4 Hz, CH arom., 1 H), 7.47-7.49 (m, CH arom., 2 H), 7.59-7.66 (m, CH arom., 6 H) ppm. ^{13}C{H} NMR (C_6D_6, 125.79 MHz): δ 117.8, 120.8, 121.5, 122.2, 125.4, 126.1, 126.7, 127.3, 127.5, 128.1, 128.4, 128.6, 130.0, 131.0, 131.2, 131.8, 133.2, 134.0, 137.4, 145.7, 148.4**,** 150.8, 152.7 ppm. ^{19}F NMR (C_6D_6, 376.3 MHz): δ -161.8, 148.8, -131.5 ppm. ^{11}B NMR (C_6D_6, 128.4 MHz): δ 29.7 ppm. Anal. Calc. for $C_{52}H_{24}B_2F_{10}O_4$ (924.36): C, 67.57; H, 2.62; Found C, 66.79; H, 2.66. Diethyl ether could not be fully removed under vacuum (10% of residual ether).

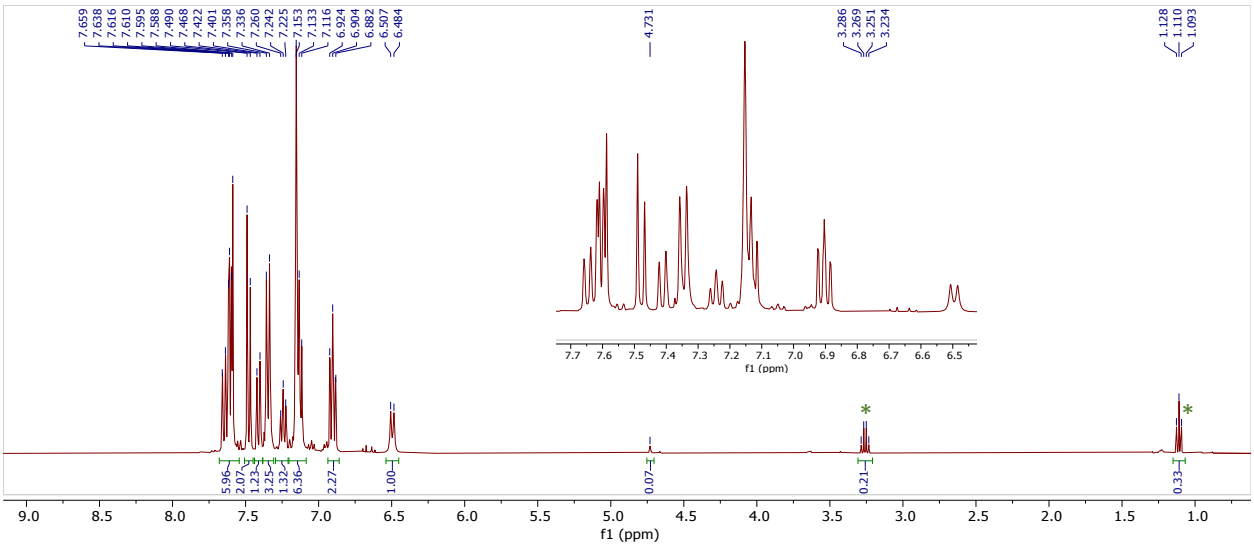

Figure S5. ^{1}H NMR spectrum of (*R,R*)-**2** in C_6D_6.(* diethyl ether)

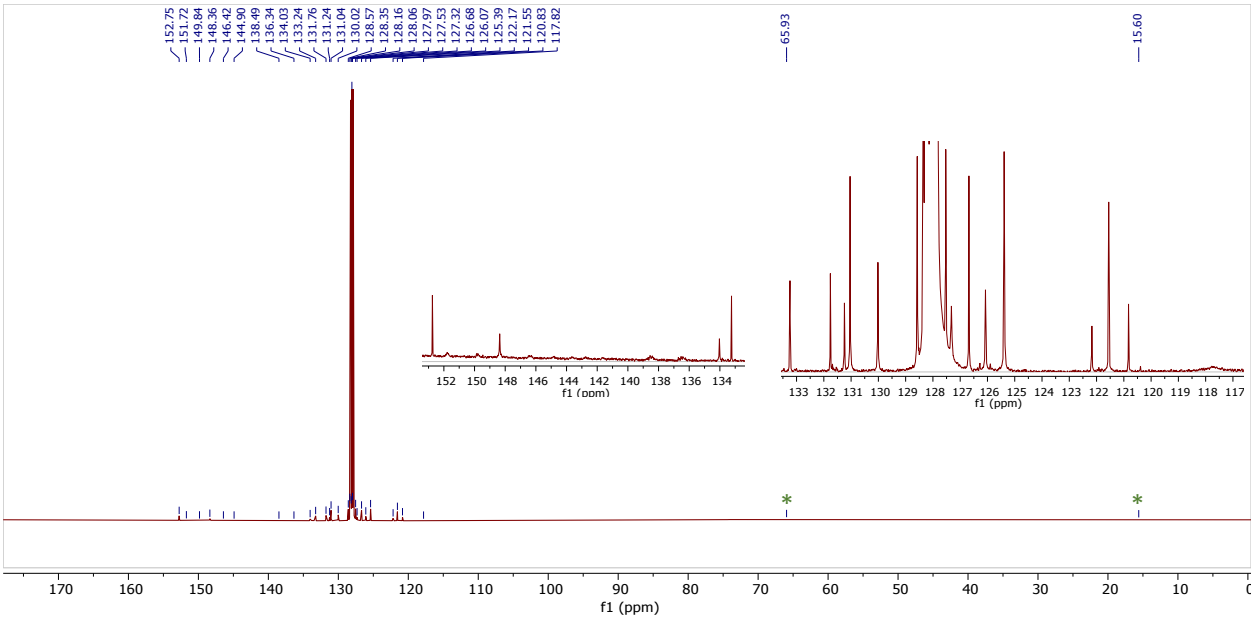

Figure S6. ^{13}C{H} NMR spectrum of (*R,R*)-**2** in C_6D_6 (* diethyl ether).

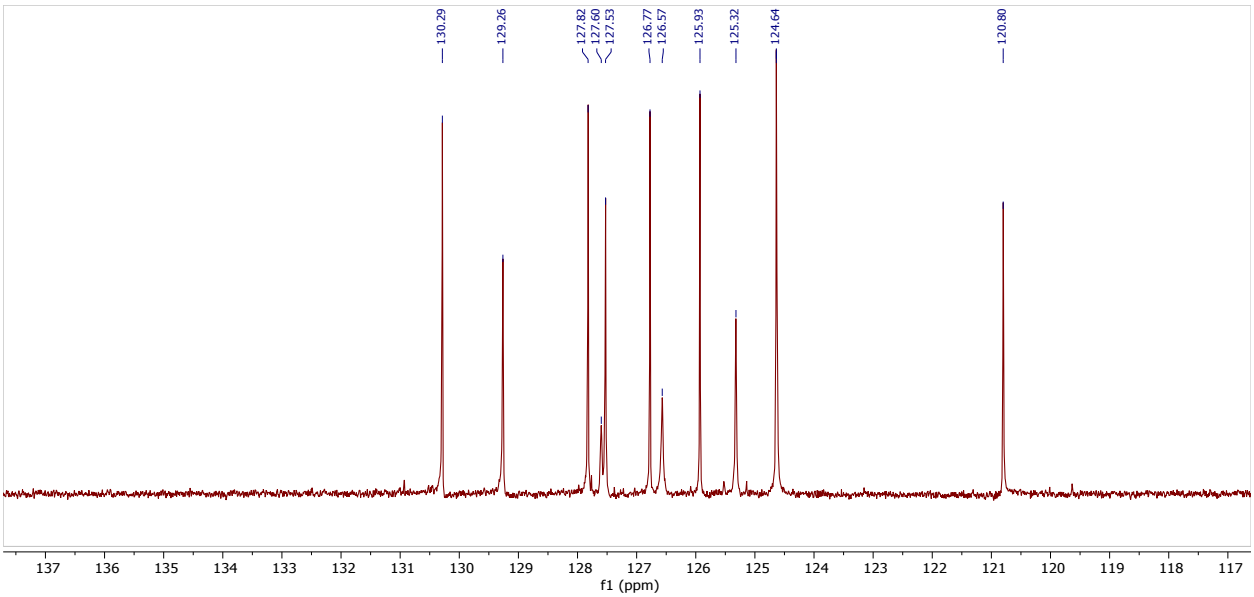

Figure S7. $^{13}C\{H\}$ (DEPT-135) NMR spectrum of (*R,R*)-**2** in C_6D_6.

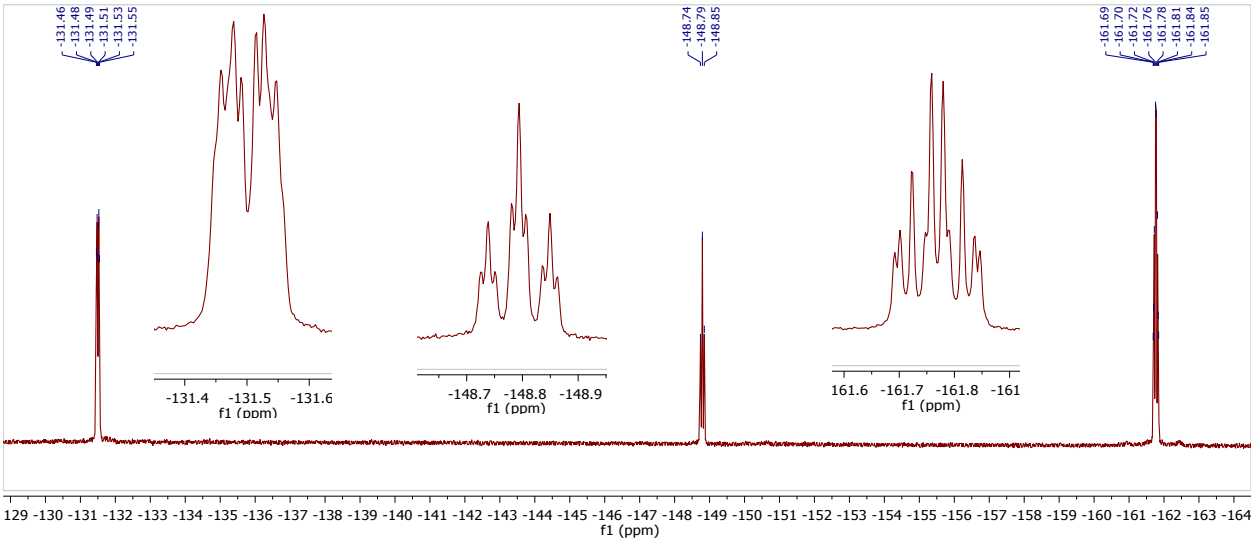

Figure S8. ^{19}F NMR spectrum of (*R,R*)-**2** in C_6D_6.

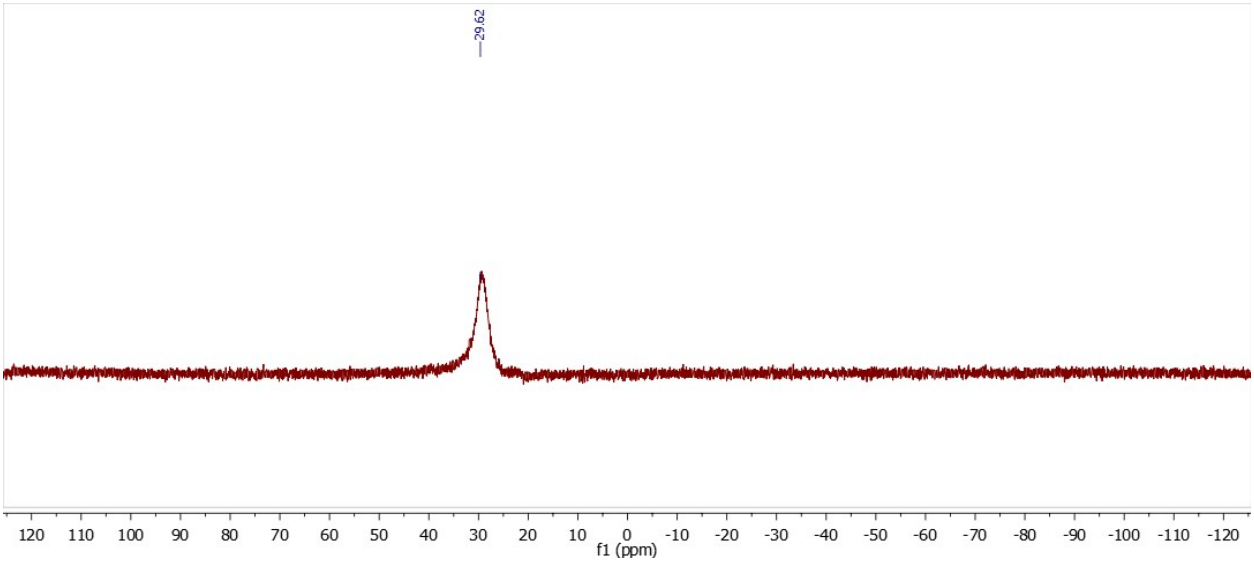

Figure S9. $^{11}B\{H\}$ NMR spectrum of (*R,R*)-**2** in C_6D_6.

2.3. Reaction of *rac*-BINOL with $C_6F_5BH_2{\cdot}SMe_2$ in diethyl ether

In the glove box, a 50 mL Schlenk flask was charged with (*rac*)-BINOL (247 mg, 0.86 mmol) and 15 mL of dry ether. To this clear solution, a solution of $C_6F_5BH_2{\cdot}SMe_2$ (220 mg, 0.91 mmol) in ether (10 mL) was slowly added and left for crystallization overnight at room temperature. The obtained crystals were washed twice with ether and dried under vacuum to give 0.51 g of a mixture of (*rac*)-BINOL, the stereoisomers (*R,R*)-**2**, (*S,S*)-**2**, (*R,S*)-**2**, (*S,R*)-**2** and an unidentified stereoisomer.

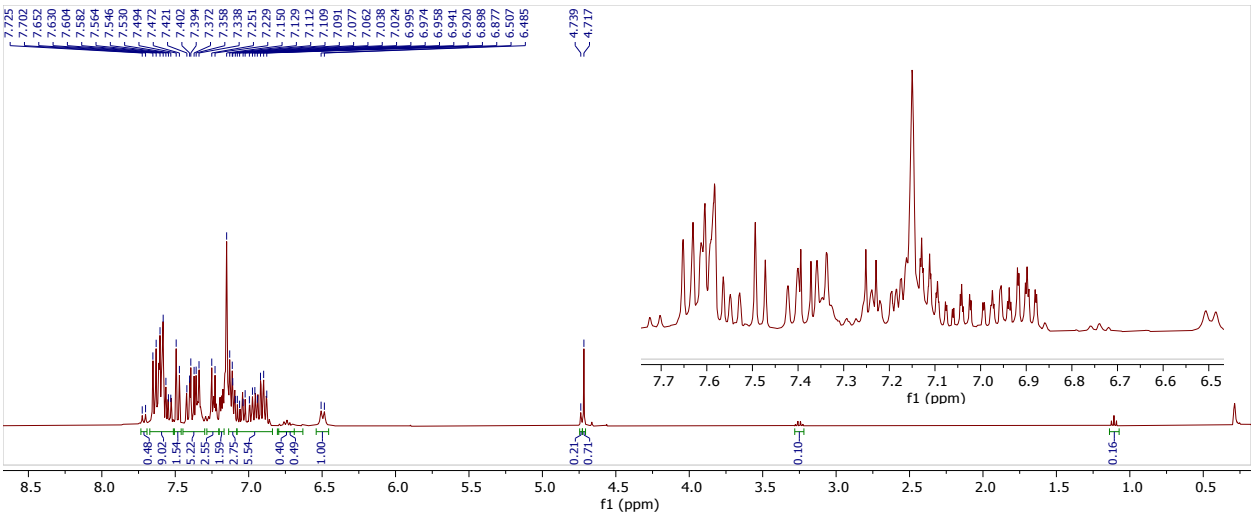

Figure S10. ^{1}H NMR spectrum of the isolated crystalline material in C_6D_6.

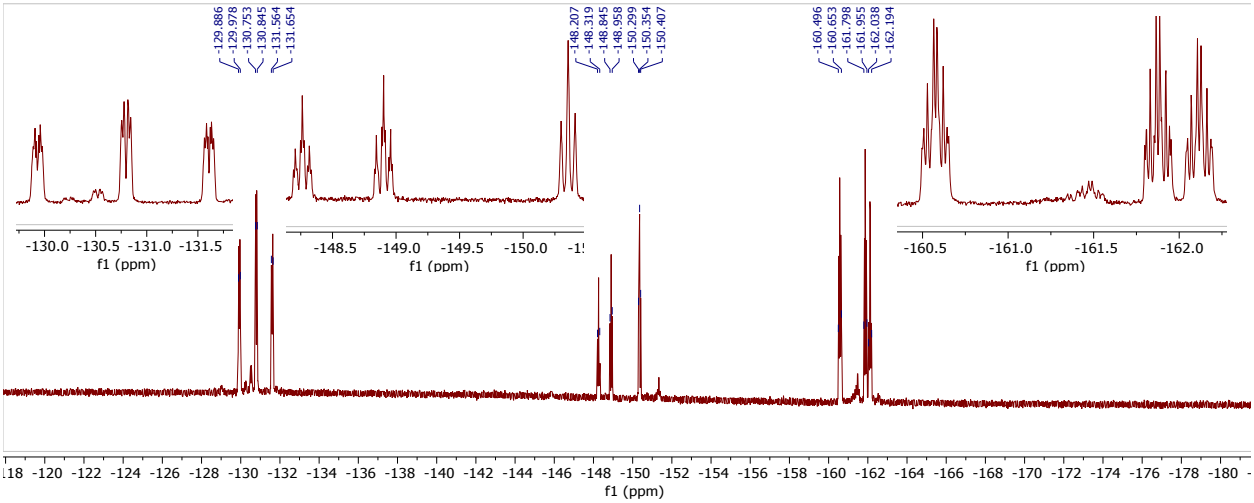

Figure S11. ^{19}F NMR spectrum of the isolated crystalline material in C_6D_6.

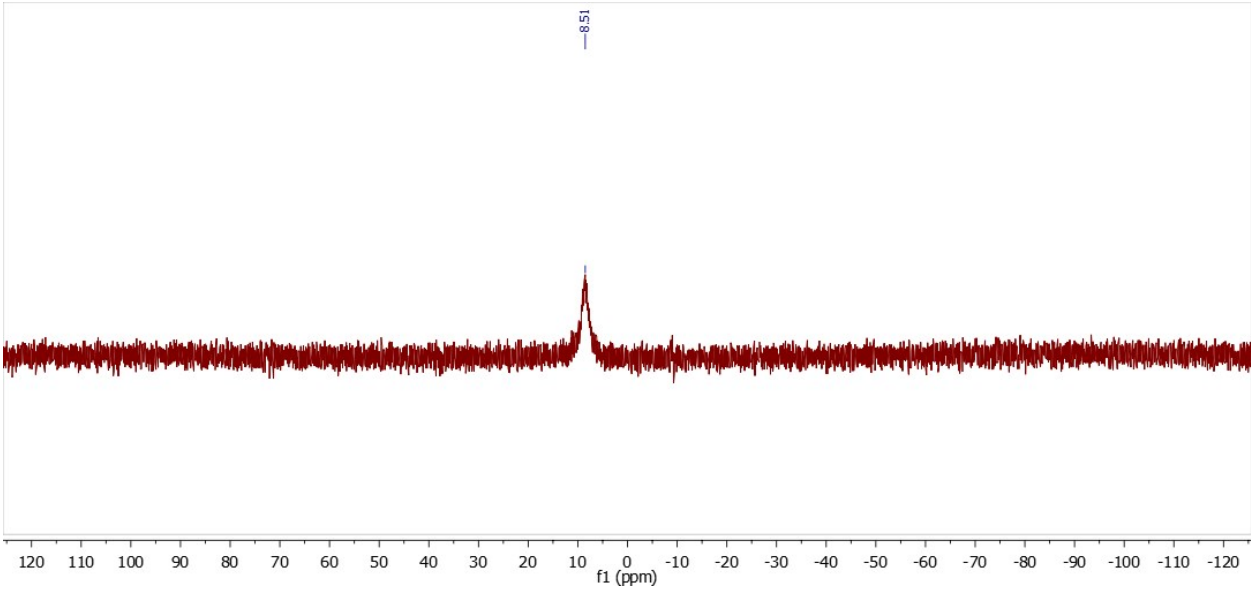

Figure S12. $^{11}B\{H\}$ NMR spectrum of the isolated crystalline material in C_6D_6.

2.4. Synthesis of (*R*)-**3**

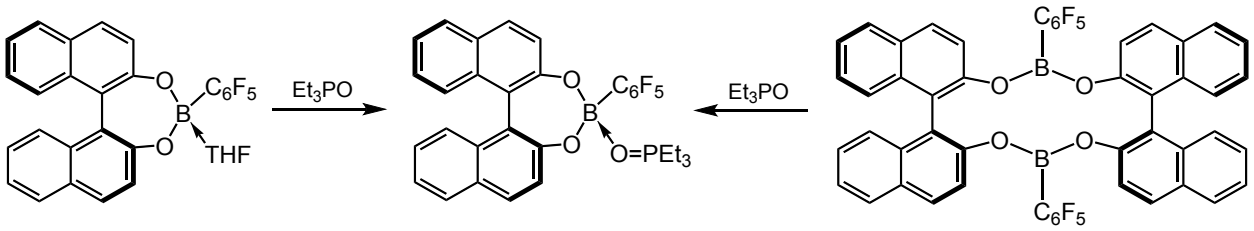

(*R*)-**1** (*R*)-**3** (*R,R*)-**2**

In the glove box, a 50 ml Schlenk flask equipped with a magnetic stir bar was charged with (*R*)-**1** (100 mg, 0.19 mmol) and 10 mL of dry toluene. To this clear solution, a solution of $O{=}PEt_3$ (25.1 mg, 0.19 mmol) in toluene (5 mL) was added and the resulting solution left for crystallization overnight at room temperature. The obtained crystals were washed twice with toluene and dried under vacuum to give ca. 60 mg (54%) of (*R*)-**3**. The reaction of (*R,R*)-**2** (88 mg, 0.095 mmol) with 2 equiv. of $O{=}PEt_3$ (25.1 mg, 0.19 mmol) proceeded similarly to give 60 mg (53%) of (*R*)-**3**. ^1H NMR (CD_2Cl_2, 400 MHz): δ 0.81-0.89 (m, CH_3, 9 H), 1.47-1.63, 1.69-1.85 (2 m, CH_2, 2 × 3 H), 7.08-7.43 (m, CH arom., 8 H), 7.75-7.92 (m, CH arom., 4 H) ppm. $^{13}C\{H\}$ NMR (CD_2Cl_2, 100.61 MHz): δ 5.3, 17.3, 122.2, 123.4,

123.5, 123.6, 124.5, 125.4, 125.6, 126.8, 127.0, 128.3, 128.4, 129.0, 130.2, 130.4, 133.5, 133.7, 137.5, 140.0, 148.6, 154.6, 155.1 ppm. ^{19}F NMR (CD_2Cl_2, 376.3 MHz): δ -133.3, -159.8, -165.4 ppm. ^{31}P NMR (CD_2Cl_2, 161.9 MHz): δ 78.2 ppm. ^{11}B NMR (CD_2Cl_2, 128.4 MHz): δ 6.0 ppm. Anal. Calc. for $C_{32}H_{37}BF_5O_3P$ (596.34): C, 64.45; H, 4.56; Found C, 64.00; H, 4.16.

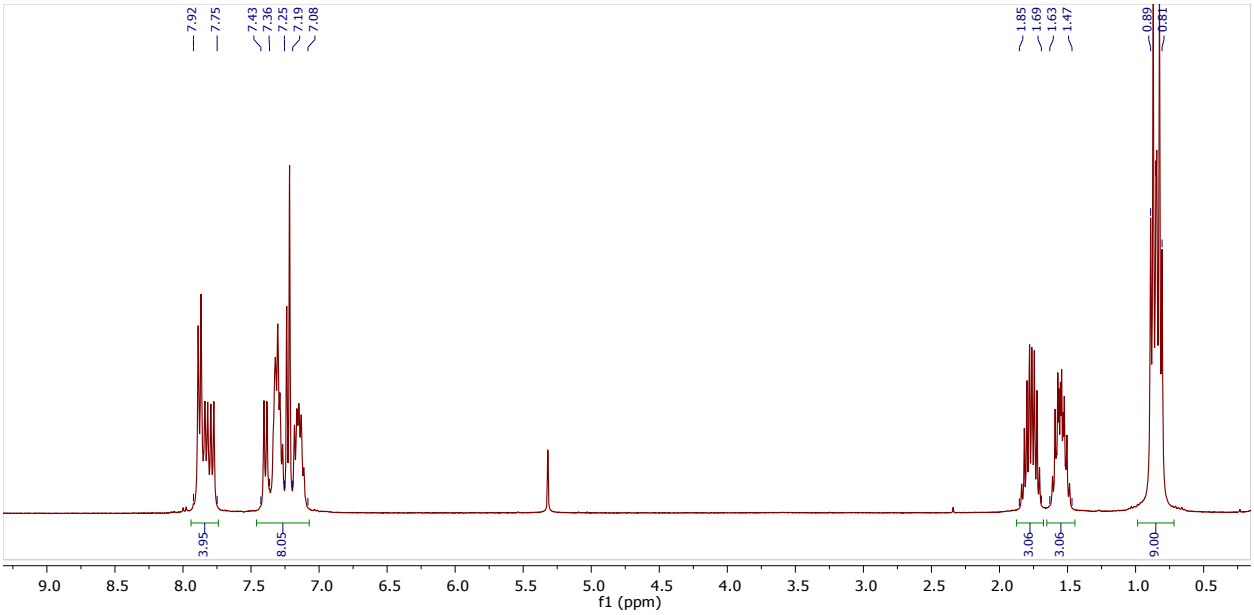

Figure S13. ^{1}H NMR spectrum of (*R*)-**3** in CD_2Cl_2.

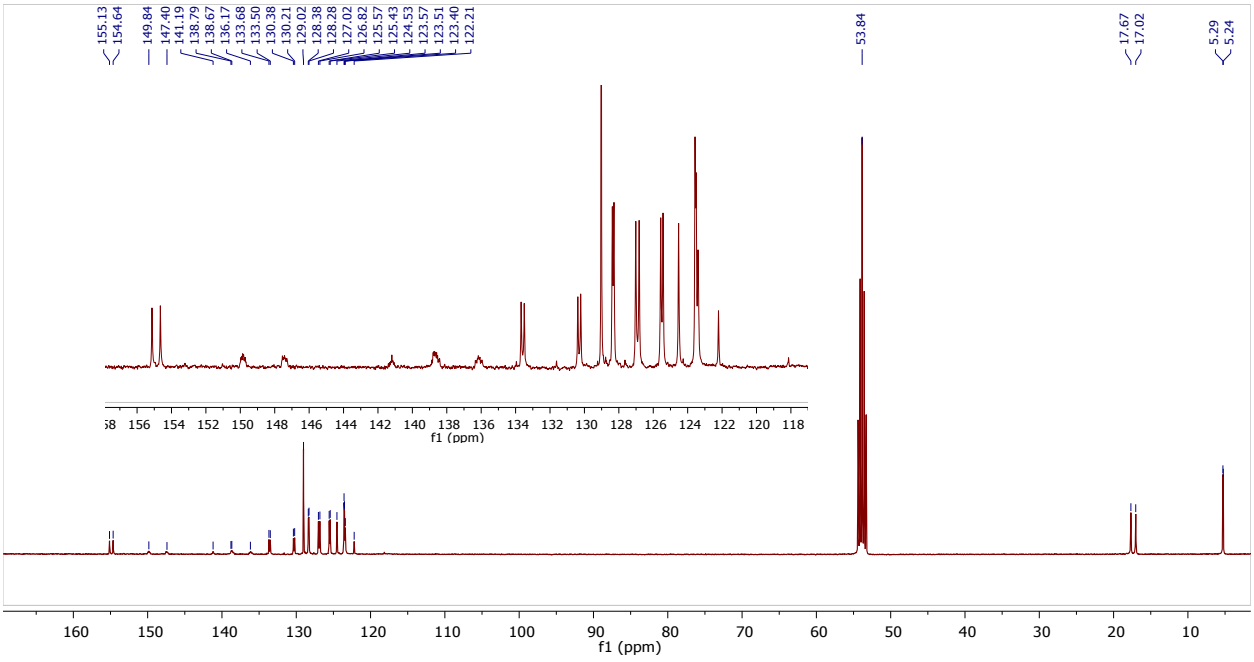

Figure S14. ^{13}C{H} NMR spectrum of (*R*)-**3** in CD_2Cl_2.

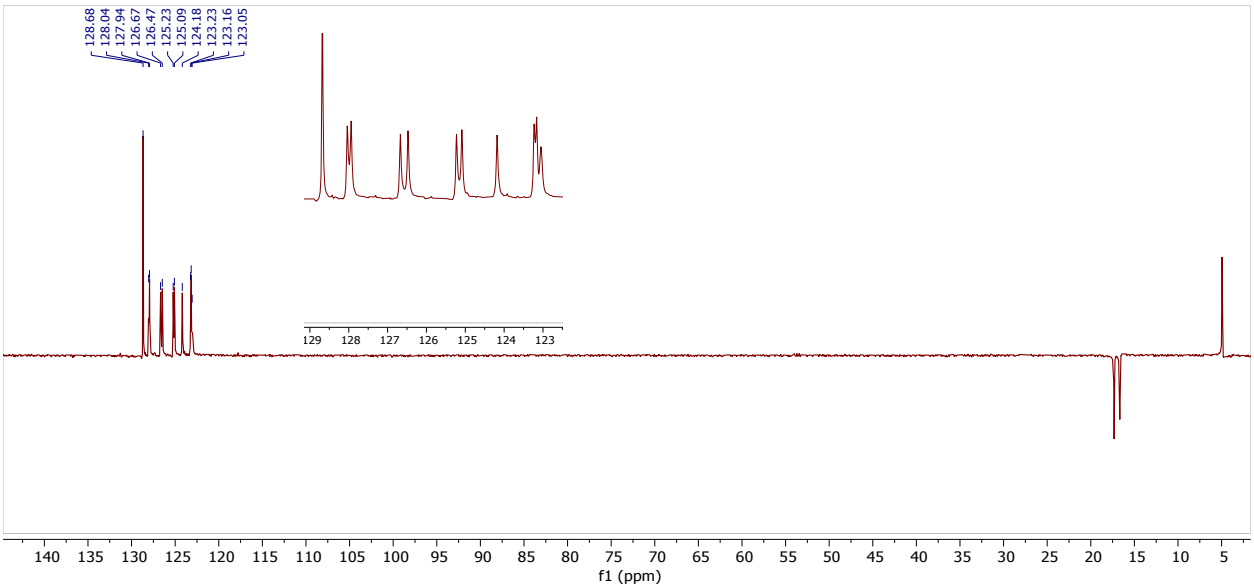

Figure S15. $^{13}C\{H\}$ (DEPT-135) NMR spectrum of (*R*)-**3** in CD_2Cl_2.

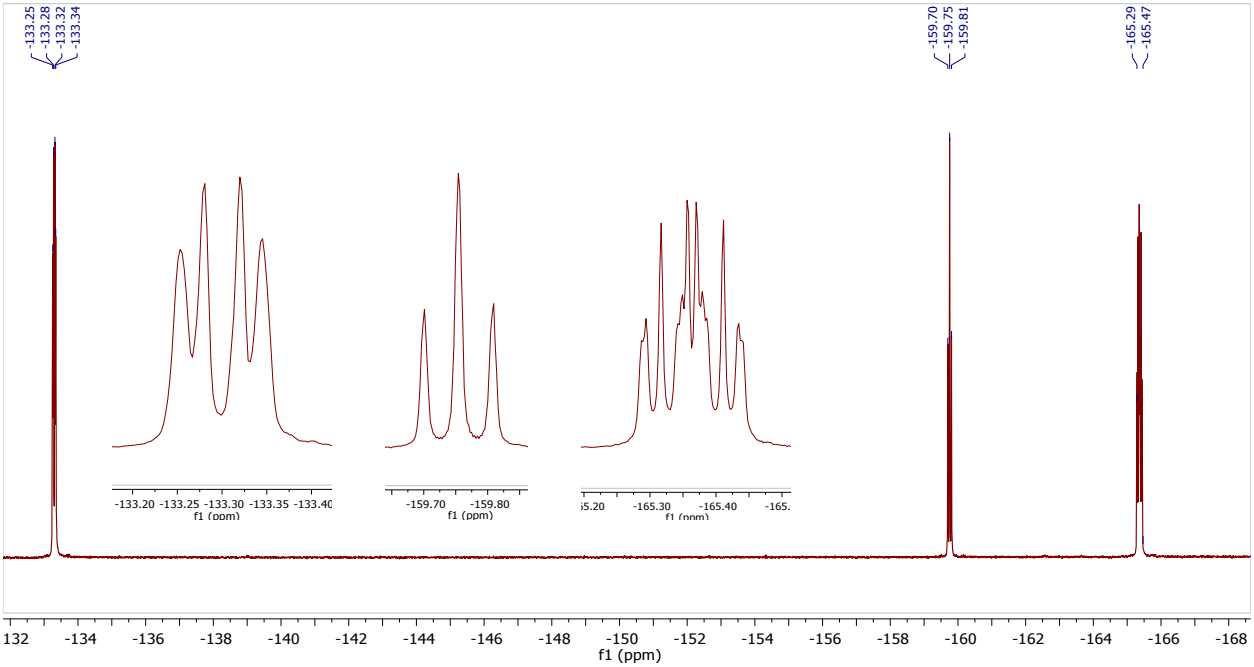

Figure S16. ^{19}F NMR spectrum of (*R*)-**3** in CD_2Cl_2.

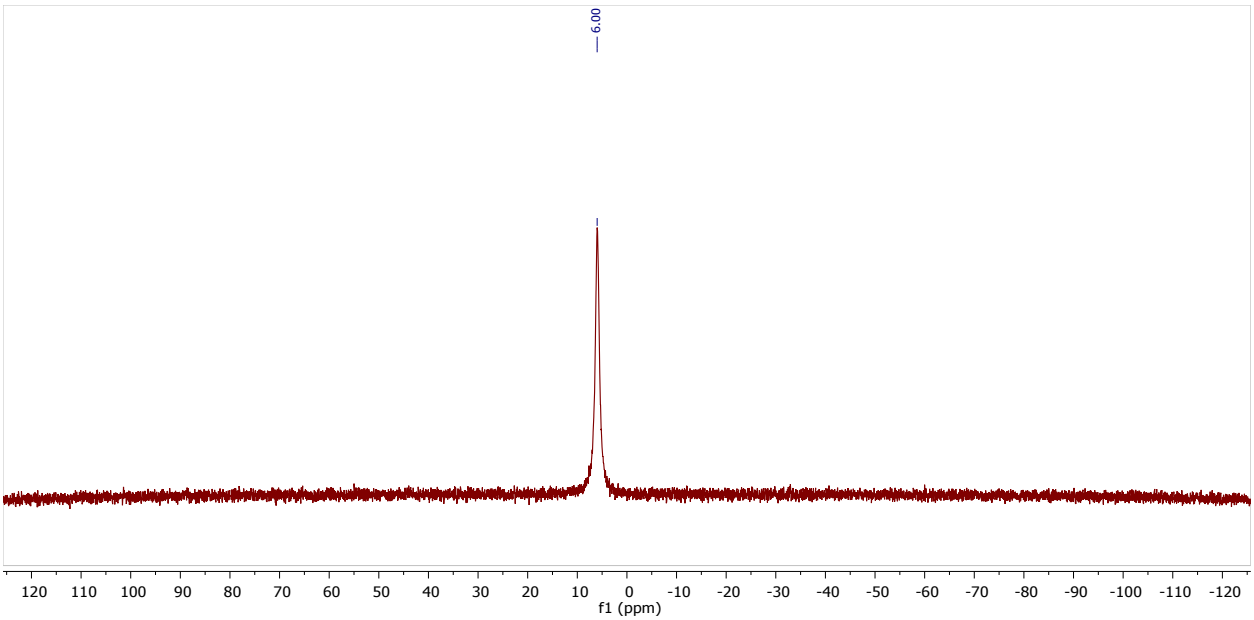

Figure S17. $^{11}B\{H\}$ NMR spectrum of (*R*)-**3** in CD_2Cl_2.

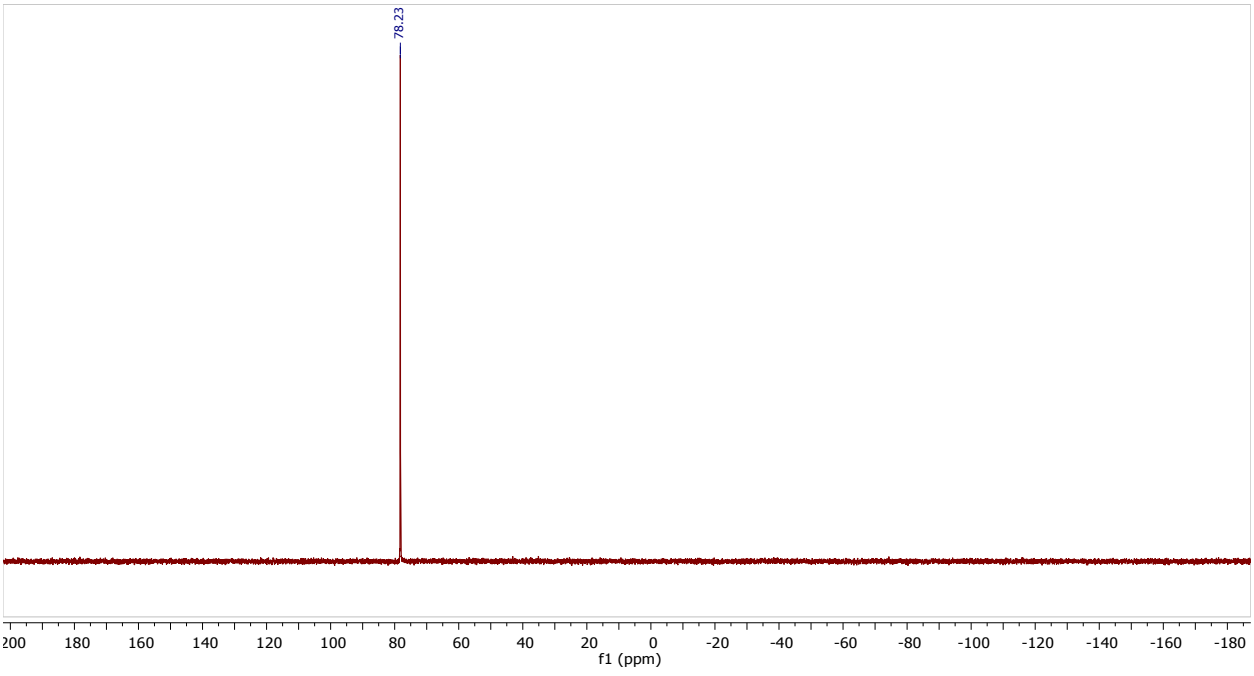

Figure S18. $^{31}P\{H\}$ NMR spectrum of (*R*)-**3** in CD_2Cl_2.

2.5. Reaction of (*R*)-**1** with PhCH=N(O)Me – Formation of (*R*)-**4**

In the glove box, a J-Young NMR tube was charged with (*R*)-**1** (68 mg, 0.13 mmol) and 0.5 mL of C_6D_6. After PhCH=N(O)Me (19 mg, 0.13 mmol) was added to the NMR tube, the resulting solution was analyzed by NMR spectroscopy. ^{1}H NMR (C_6D_6, 400 MHz): δ 1.40 (CH_2), 2.92 (s, CH_3), 3.54 (OCH_2), 6.37 (CH), 6.80-6.94 (CH arom., 5 H), 7.09 (t, J_{H-H} = 8 Hz, CH arom., 2 H), 7.43 (br, C-H arom., 2 H), 7.52-7.63 (CH arom., 6 H), 7.74 (d, J_{H-H} = 8 Hz, CH arom., 2 H) ppm. ^{13}C{H} NMR (C_6D_6,125.79 MHz): δ 25.8, 51.3, 67.9, 123.0, 123.3, 123.7, 125.8, 127.5, 128.4, 128.4, 128.8, 129.3, 130.5, 132.3, 133.8, 134.7, 137.6, 140.3, 149.1, 155.0, 160.2 ppm. ^{11}B NMR (C_6D_6, 128.4 MHz): δ 7.6 ppm. ^{19}F NMR (C_6D_6, 161.9 MHz): δ -164.4, -158.1, -131.6 ppm.

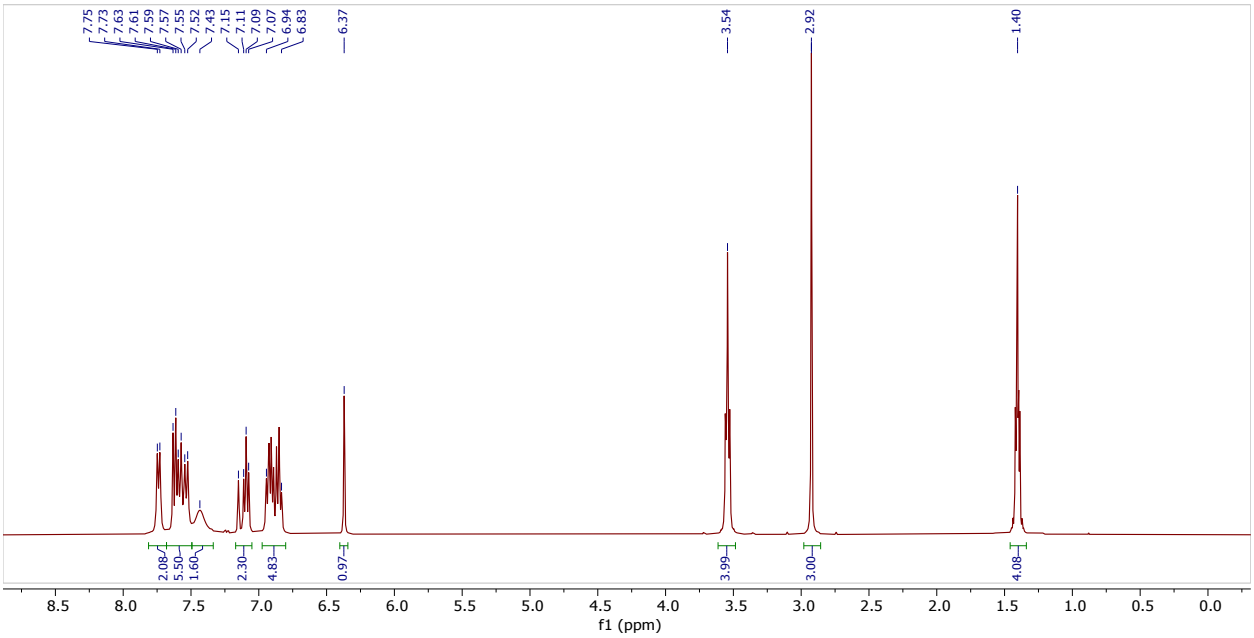

Figure S19. ^{1}H NMR spectrum of the mixture in C_6D_6.

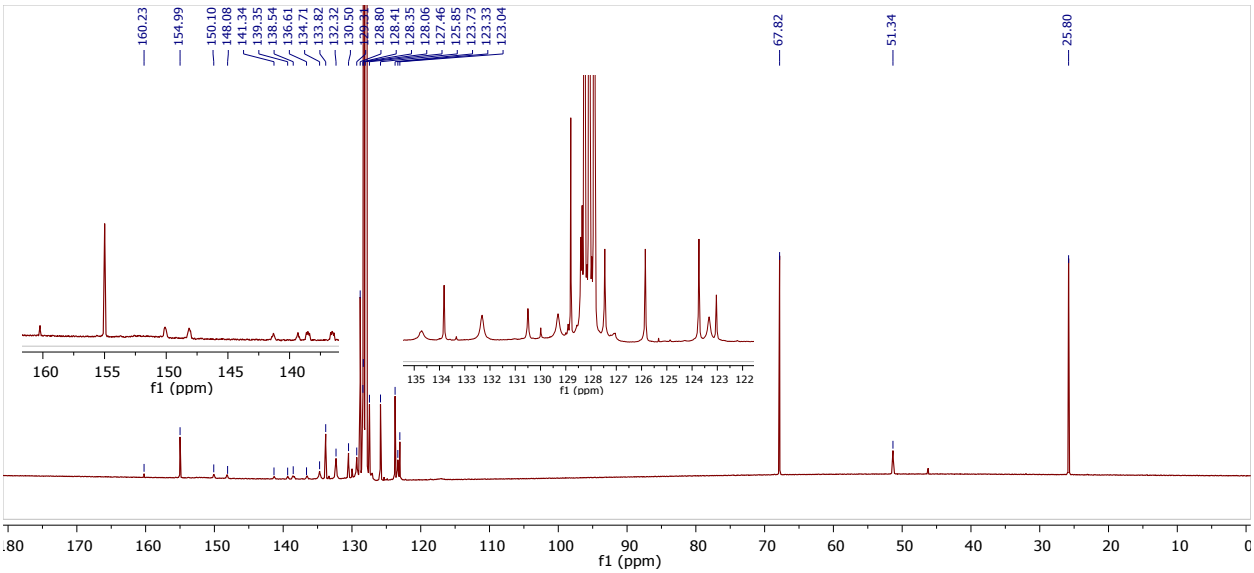

Figure S20. $^{13}C\{H\}$ NMR spectrum of the mixture in C_6D_6.

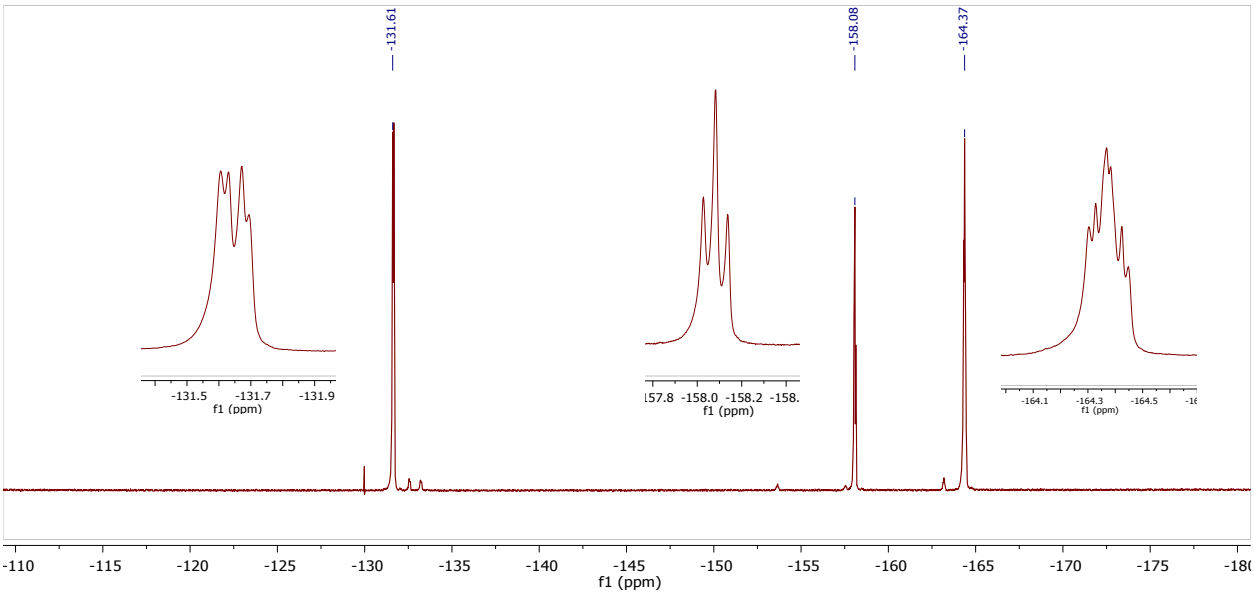

Figure S21. ^{19}F NMR spectrum of the mixture in C_6D_6.

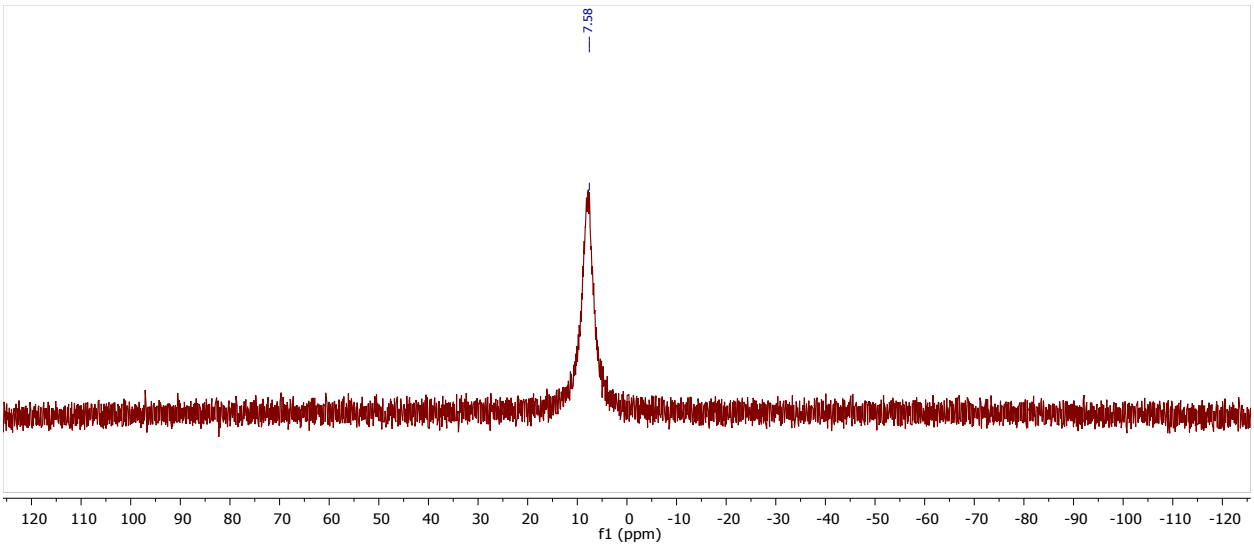

Figure S22. $^{11}B\{H\}$ NMR spectrum of the mixture in C_6D_6.

2.6. Reaction of (*R,R*)-**2** with PhCH=N(O)Me – Formation of (*R*)-**4**

In the glove box, a J-Young NMR tube was charged with (*R,R*)-**2** (68 mg, 0.07 mmol) and 0.5 mL of C_6D_6. After 2 equiv. of PhCH=N(O)Me (19 mg, 0.14 mmol) were added to the NMR tube, the resulting solution was analyzed by NMR spectroscopy. ^1H NMR (C_6D_6, 400 MHz): δ 2.87 (s, CH_3, 3 H), 6.18 (s, CH, 1 H), 6.79-6.95 (m, CH arom., 5 H), 7.10 (t, J_{H-H} = 8 Hz, CH arom., 2 H), 7.43 (br, C-H arom., 2 H), 7.55-7.66 (m, CH arom., 8 H) ppm. $^{13}C\{H\}$ NMR (C_6D_6,125.79 MHz): δ 51.0, 123.0, 123.3, 123.7, 125.8, 126.4, 127.5, 128.4, 129.3, 130.5, 132.6, 133.8, 135.3, 137.7, 140.3, 152.1, 153.7, 155.0, 160.4 ppm. ^{11}B NMR (CD_2Cl_2 (128.4 MHz): δ 7.9 ppm. ^{19}F NMR (C_6D_6, 161.9 MHz): δ -164.4, -158.1, -131.6 ppm.

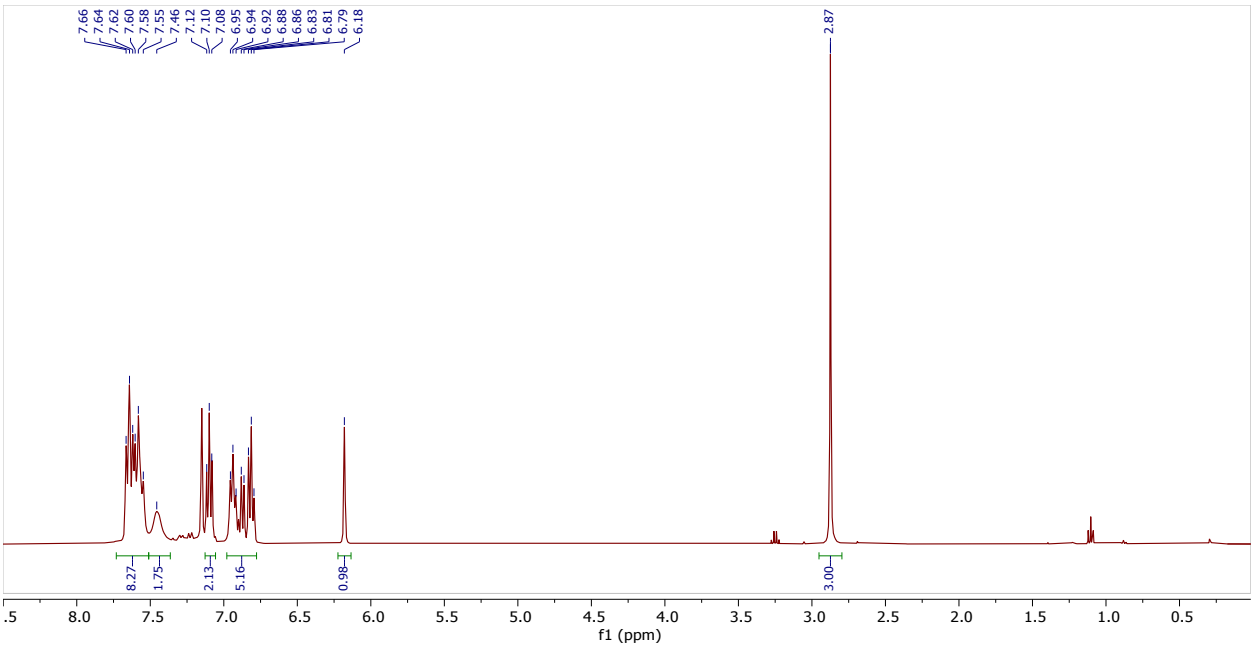

Figure S23. ^{1}H NMR spectrum of the mixture in C_6D_6.

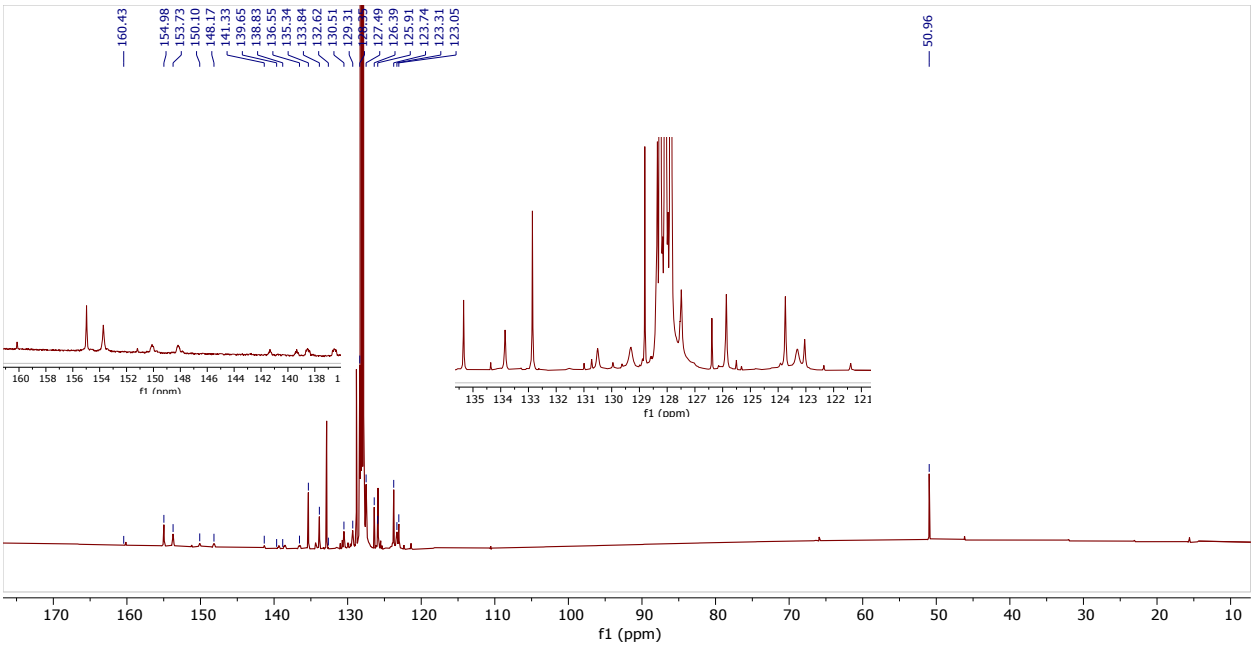

Figure S24. $^{13}C\{H\}$ NMR spectrum of the mixture in C_6D_6.

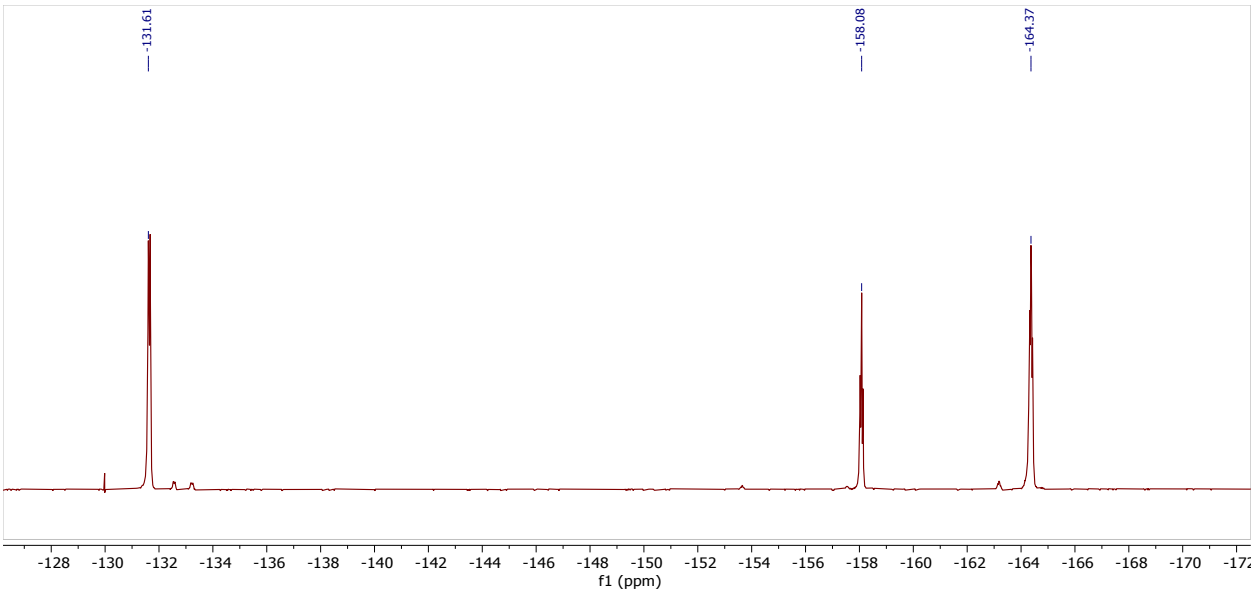

Figure S25. ^{19}F NMR spectrum of the mixture in C_6D_6.

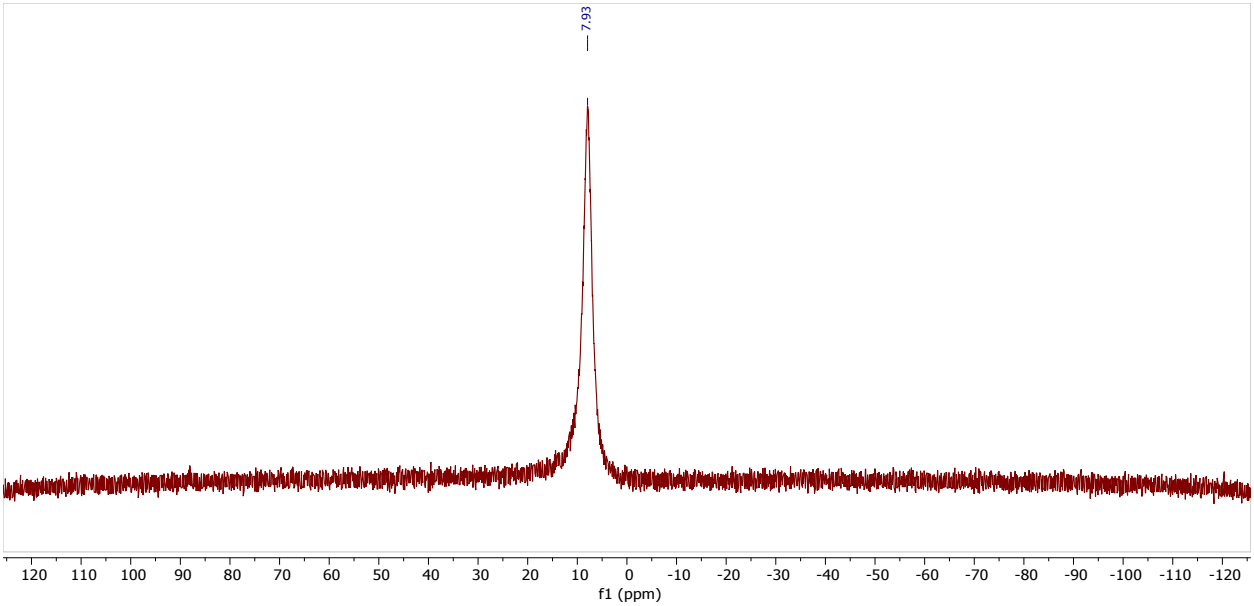

Figure S26. $^{11}B\{H\}$ NMR spectrum of the mixture in C_6D_6.

2.7. Synthesis of (*R,R,R*)-**5**

In the glove box, a 50 ml Schlenk flask was charged with (*R*)-BINOL (1 g, 3.5 mmol) and dry diethyl ether (20 mL). To this clear solution, $Me_2S{\bullet}BH_3$ (0.25 ml, 2.6 mmol) dissolved in diethyl ether (5 mL) was slowly added. The resulting solution was left for crystallization overnight at room temperature. The obtained crystalline material was washed twice with

diethyl ether and dried under vacuum to give 1 g (97%) of (*R,R,R*)-**5**. The obtained NMR spectroscopic data are consistent with those reported in the literature [3].

2.8. Synthesis of (*R*)-**6**

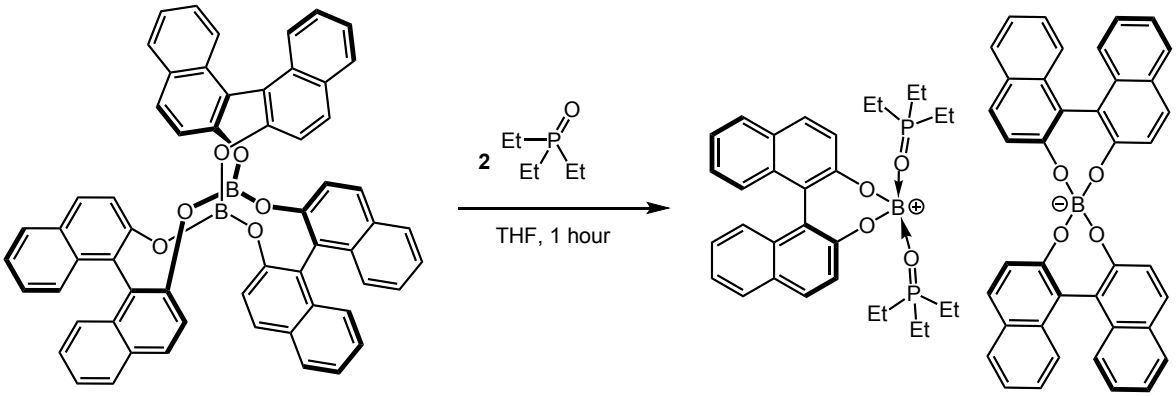

In the glove box, a 50 ml Schlenk flask equipped with a magnetic stir bar was charged with (*R,R,R*)-**5** (300 mg, 0.34 mmol) and of dry THF (15 mL). To this clear solution, $O{=}PEt_3$ (92 mg, 0.68 mmol) dissolved in THF (5 mL) was added. The resulting solution was left overnight at room temperature for crystallization. The obtained precipitate was washed once with THF and dried under vacuum to give 0.28 g (70%) of (*R*)-**6**. ^{1}H NMR (C_6D_6, 400 MHz): δ -0.07-0.01 (m, CH_3, 18 H), 0.93-1.08 (m, CH_2, 12 H), 6.73 (d, $^3J_{H\text{-}H}$ = 8.7 Hz, CH arom., 2 H), 6.86 (t, $^3J_{H\text{-}H}$ = 7.7 Hz, CH arom., 2 H), 6.98 (t, $^3J_{H\text{-}H}$ = 7.2 Hz, CH arom., 4 H), 7.05-7.08 (m, CH arom., 2 H), 7.11-7.13 (m, CH arom., 3 H), 7.33 (d, $^3J_{H\text{-}H}$ = 8.6 Hz, CH arom., 2 H), 7.39 (d, $^3J_{H\text{-}H}$ = 8.8 Hz, CH arom., 2 H), 7.51-7.62 (m, CH arom., 11 H), 7.72 (d, $^3J_{H\text{-}H}$ = 8.0 Hz, CH arom., 5 H), 7.79 (d, $^3J_{H\text{-}H}$ = 8.7 Hz, CH arom., 4 H) ppm. ^{13}C{H} NMR (C_6D_6, 125.79 MHz): δ 4.2, 16.5, 122.5, 122.8, 123.0, 123.2, 123.8, 124.9, 125.4, 125.8, 127.0, 127.9, 128.3, 128.4, 128.6, 129.1, 129.99, 130.3, 133.2, 133.96, 153.2, 156.6 ppm. ^{31}P NMR (C_6D_6, 161.9 MHz): δ 82.6 ppm. ^{11}B NMR (C_6D_6, 128.4 MHz): δ 2.1, 8.3 ppm. Calc. for $C_{74}H_{70}B_2O_8P_2$ (1170.93): C, 75.91; H, 6.03; Found C, 74.47; H, 5.99.

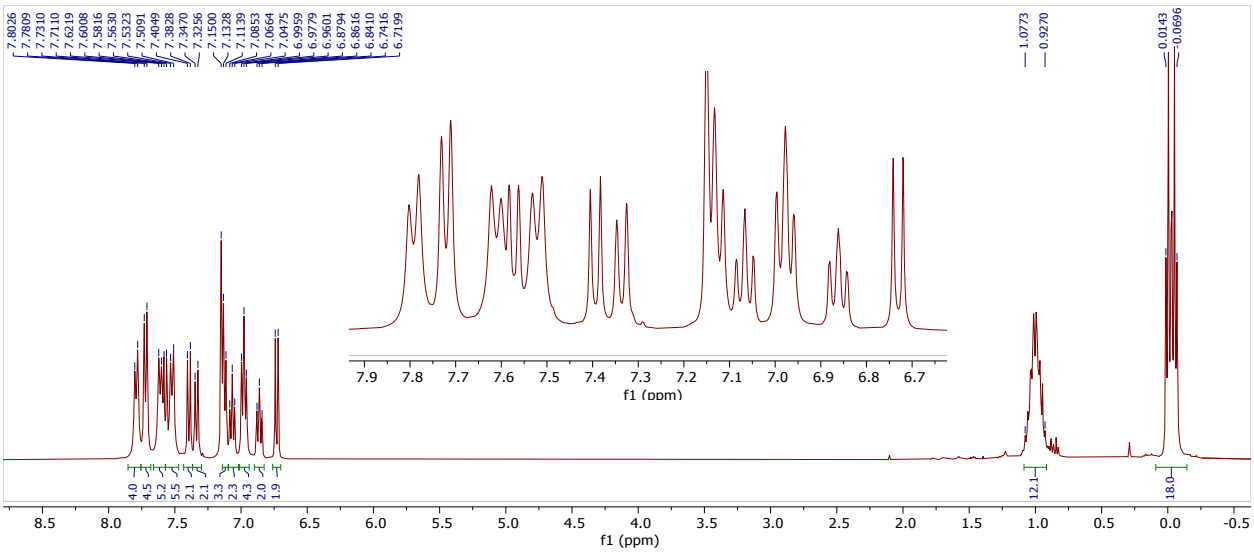

Figure S27. ^{1}H NMR spectrum of (*R*)-**6** in C_6D_6.

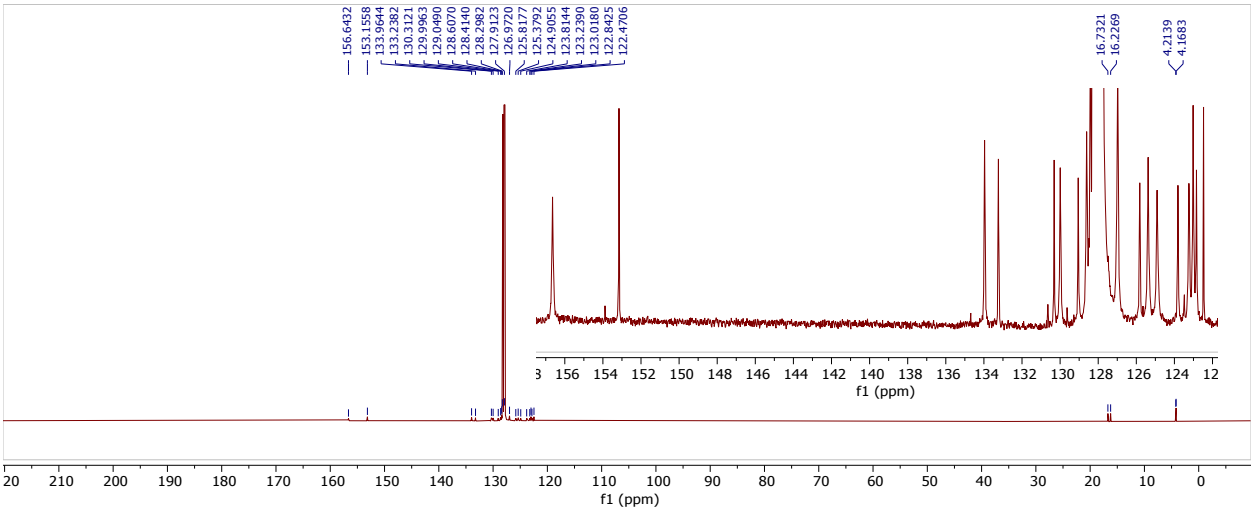

Figure S28. ^{13}C{H} NMR spectrum of (*R*)-**6** in C_6D_6.

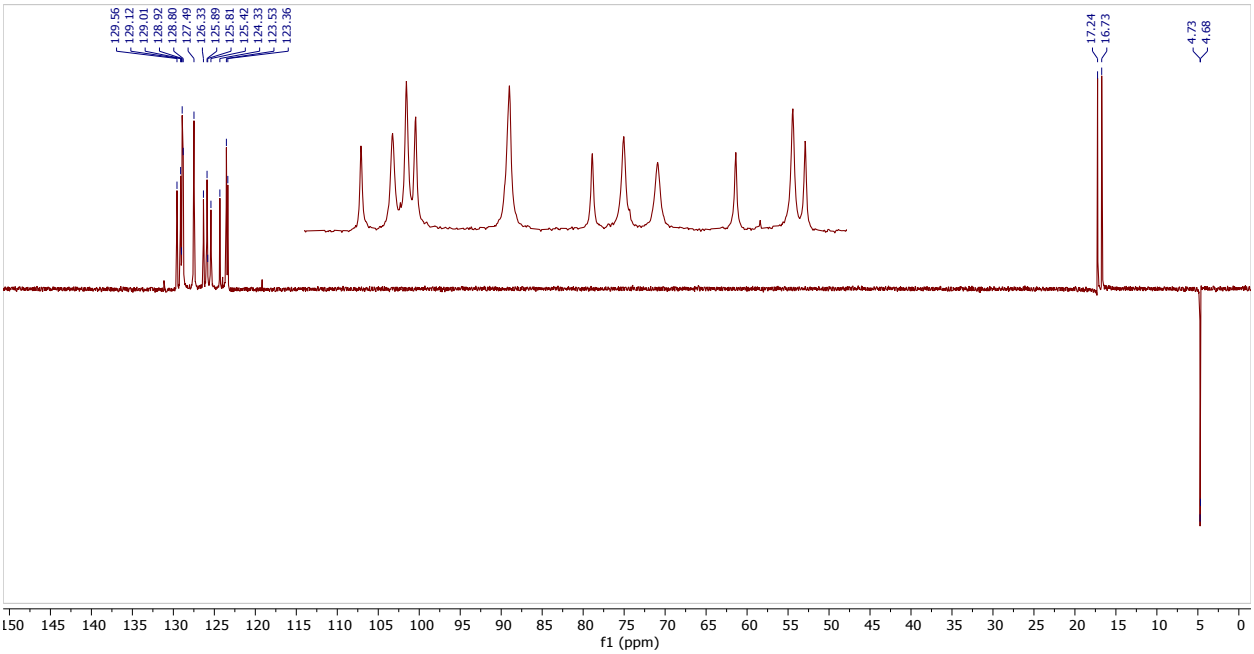

Figure S29. $^{13}C\{H\}$ (DEPT-135) NMR spectrum of (*R*)-**6** in C_6D_6.

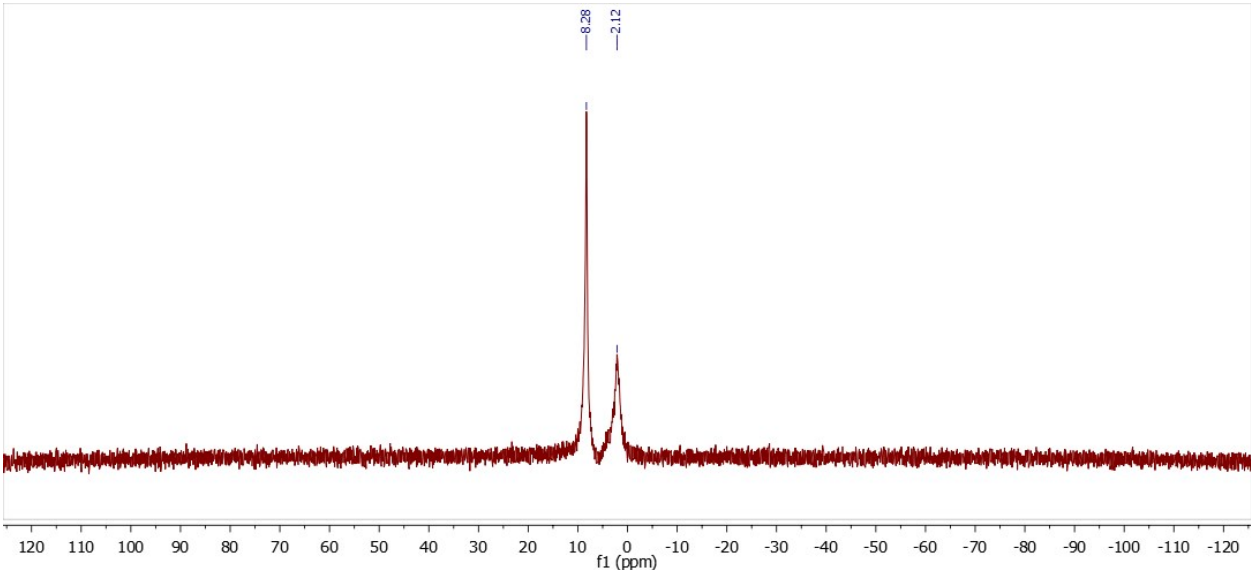

Figure S30. $^{11}B\{H\}$ NMR spectrum of (*R*)-**6** in C_6D_6.

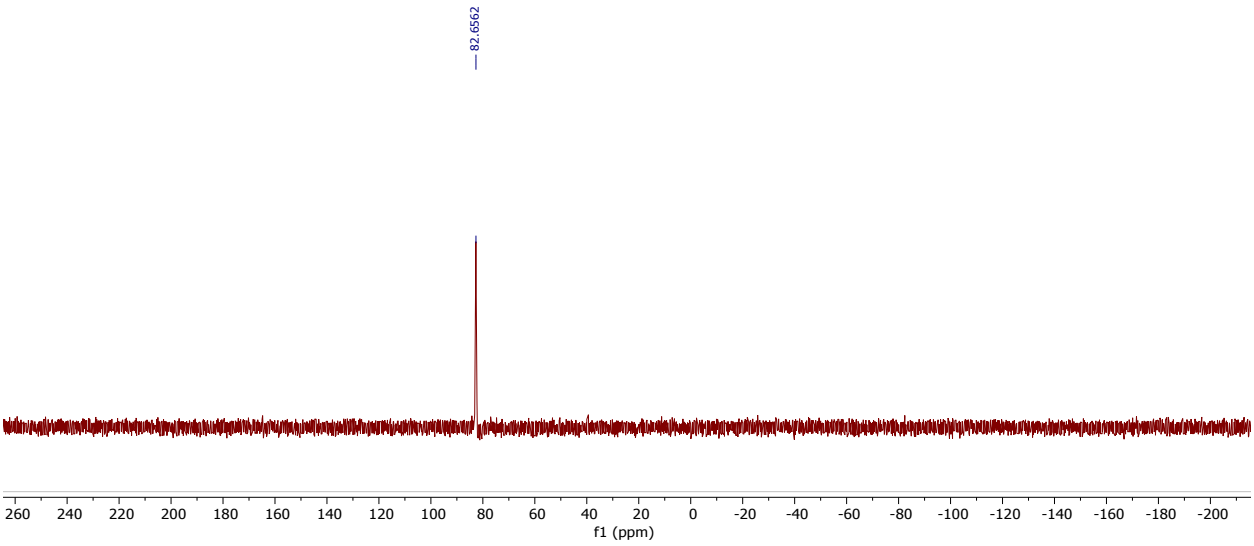

Figure S31. $^{31}P\{H\}$ NMR spectrum of (*R*)-**6** in C_6D_6.

2.8. Synthesis of (*R*)-**7**

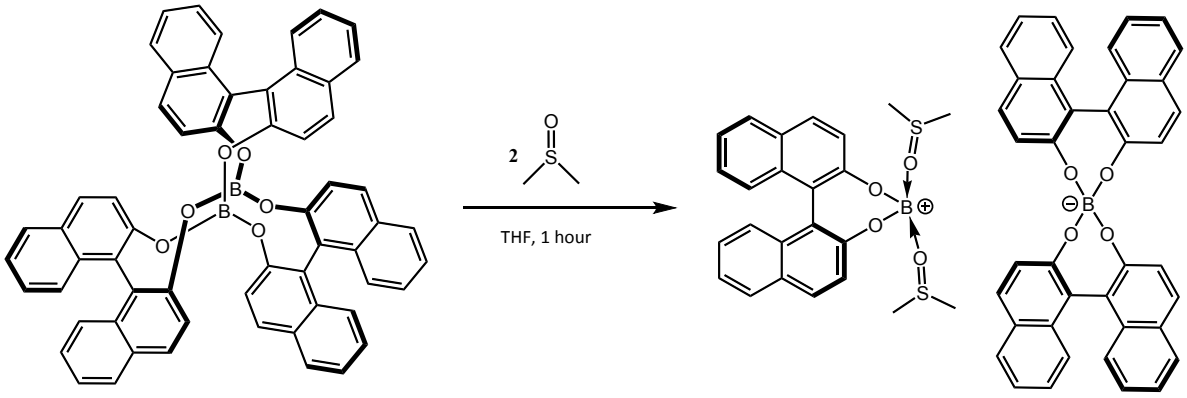

Under nitrogen, a 50 ml Schlenk flask equipped with a magnetic stir bar was charged with (*R,R,R*)-**5** (300 mg, 0.34 mmol) and THF (15 mL). To this solution, anhydrous DMSO (53 mg, 0.68 mmol) dissolved in THF (5 mL) was added and left at room temperature for crystallization. The obtained precipitate was washed twice with THF (2 mL) and dried under vacuum to give 300 mg (83%) of (*R*)-**7**. ^{1}H NMR [DMSO-D_6, 400 MHz]: δ 2.54 (s, CH_3, 12 H), 7.11-7.42 (m, CH arom., 26 H), 7.92-8.03 (m, CH arom., 12 H) ppm. $^{13}C\{H\}$ NMR (DMSO-D_6, 125.79 MHz): δ 40.4 (CH_3), 121.0, 121.8, 122.4, 122.4, 124.0, 124.4, 124.5, 124.9, 125.8, 125.9, 128.1, 128.2, 128.4, 129.0, 129.8, 130.0, 132.2, 132.8, 152.2,

156.0 ppm. ^{11}B NMR (DMSO-D_6, (128.4 MHz): δ 4.2, 8.1 ppm. Calc. for $C_{66}H_{52}B_2O_8S_2$ (1058.87): C, 74.87; H, 4.95; Found C, 73.58; H, 5.08.

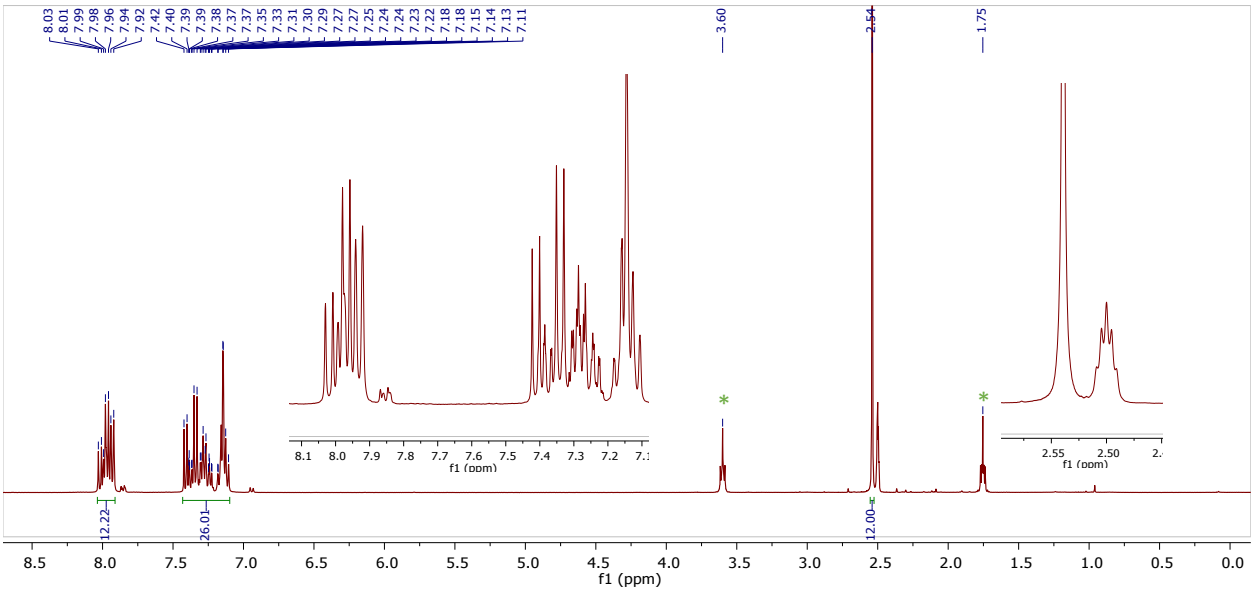

Figure S32. ^{1}H NMR spectrum of (*R*)-**7** in DMSO-D_6. (* represents THF)

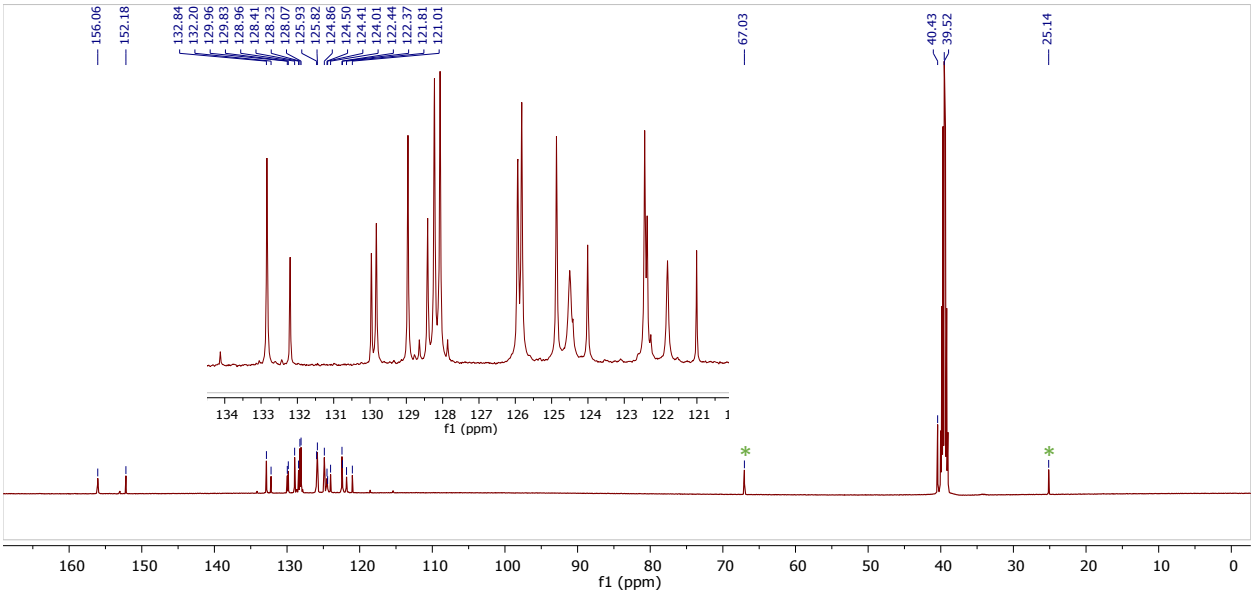

Figure S33. ^{13}C{H} NMR spectrum of (*R*)-**7** in DMSO-D_6. (* represents THF)

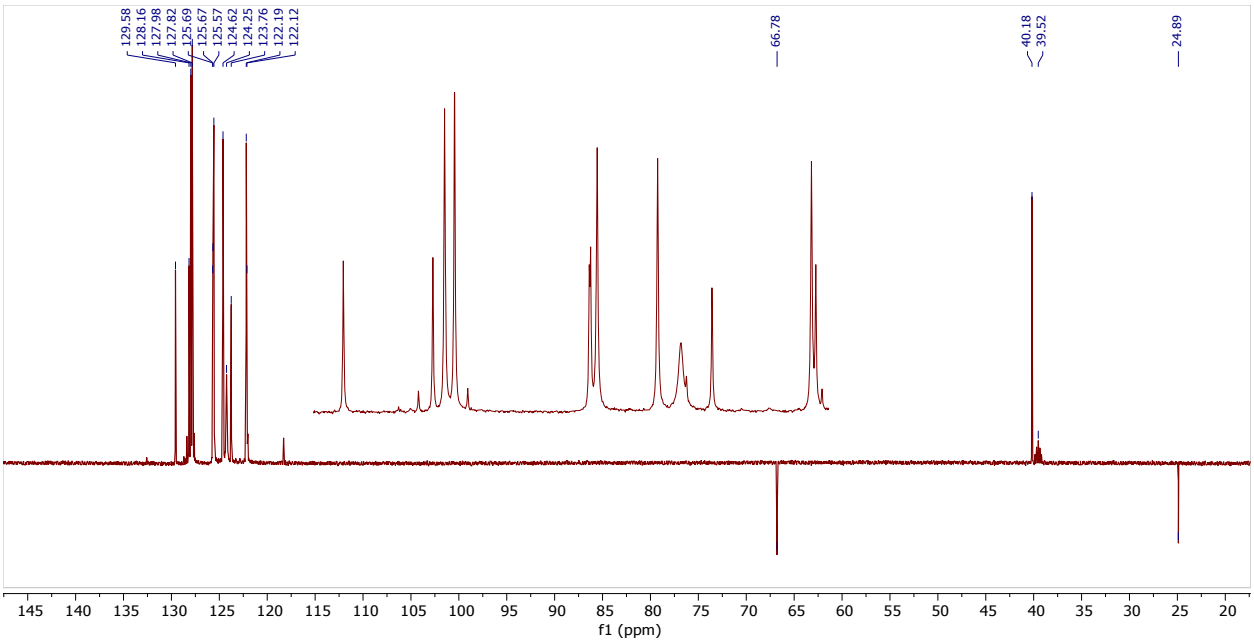

Figure S34. $^{13}C\{H\}$ (DEPT-135) NMR spectrum of (*R*)-**7** in DMSO-D_6.

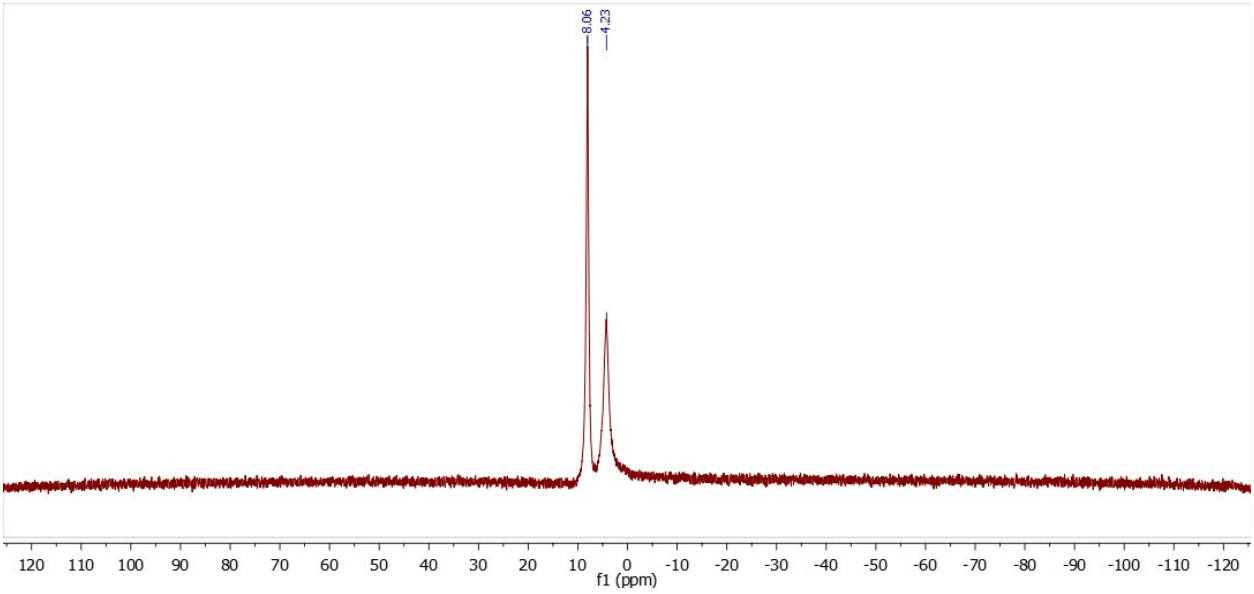

Figure S35. $^{11}B\{H\}$ NMR spectrum of (*R*)-**7** in DMSO-D_6.

2.9. Synthesis of (*R*)-**8**

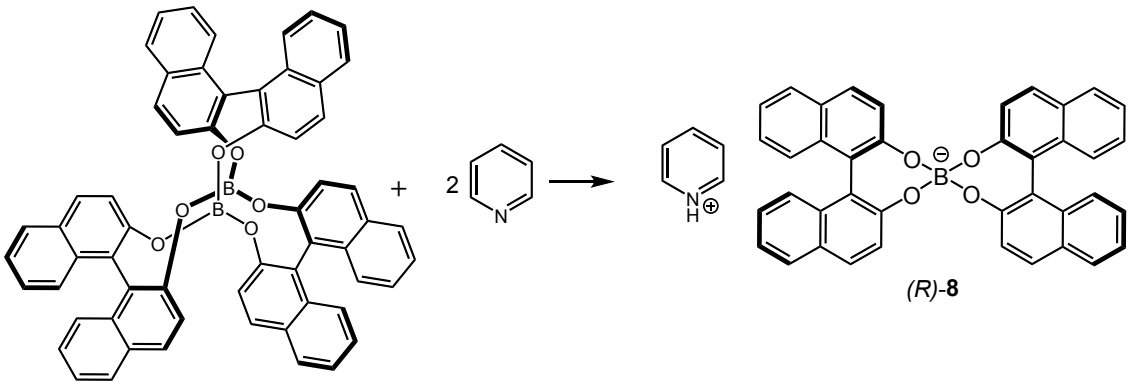

(R,R,R)-**5**

(R)-**8**

In the glove box, a 50 mL Schlenk flask equipped with a magnetic stir bar was charged with (*R,R,R*)-**5** (100 mg, 0.114 mmol) and dry THF (10 mL). To this clear solution, anhydrous pyridine (18 mg, 0.228 mmol) dissolved in THF (5 mL) was added and the resulting solution left for ca. 3 days at room temperature for crystallization. The obtained crystals were washed once with THF and dried under vacuum to give 58 mg of (*R*)-**8** [77% based on (*R,R,R*)-**5**)]. ^{1}H NMR (CD_2Cl_2, 400 MHz): 7.01 (br, CH-pyridine, 2 H) 7.10-7.14 (m, CH arom., 4 H), 7.21 (d, $^{3}J_{H-H}$ = 8 Hz, CH arom., 4 H), 7.29 (t, $^{3}J_{H-H}$ = 8 Hz, CH arom., 4 H), 7.35(s, 2 H), 7.55 (m, CH arom., 4 H), 7.63 (br, CH-pyridine, 1 H), 7.83- 7.87 (m, CH arom., 6H), 7.91-7.94 (d, $^{3}J_{H-H}$ = 8 Hz, CH arom., 4 H), 7.63 (br, CH-pyridine, 2 H) ppm. ^{13}C{H} NMR (CD_2Cl_2,125.79 MHz): δ. ^{11}B NMR (CD_2Cl_2 (128.4 MHz): δ 8.2 ppm.

IR (solid) $\tilde{\nu}_{(N-H)}$ = 3245 cm^{-1} (broad).

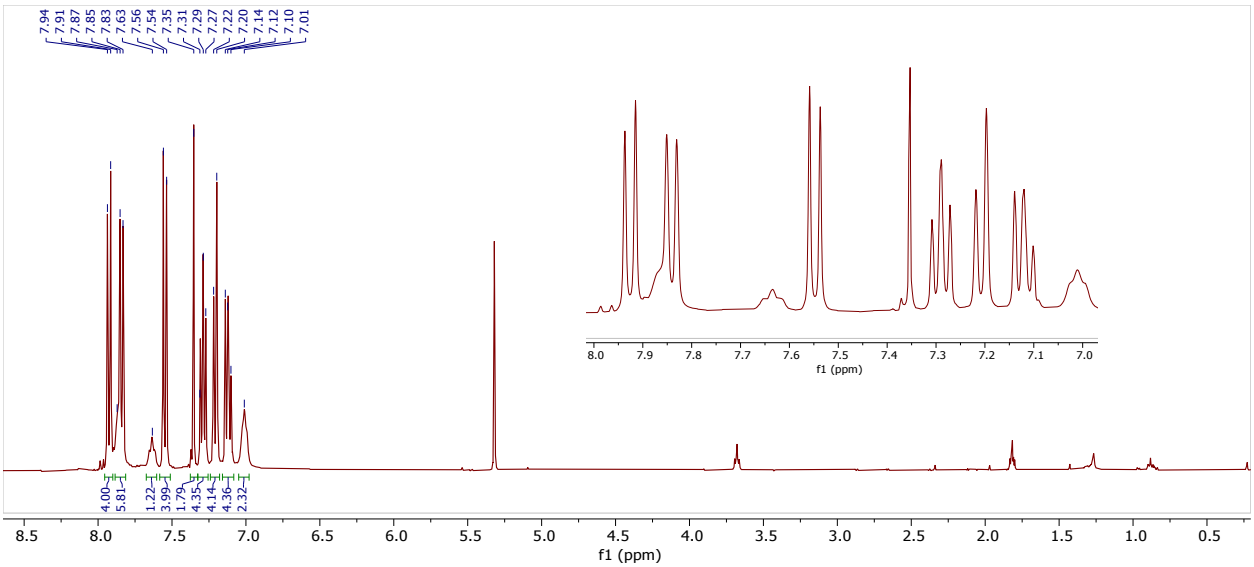

Figure S36. ^{1}H NMR spectrum of (*R*)-**8** in CD_2Cl_2 (* THF; * C_6H_6).

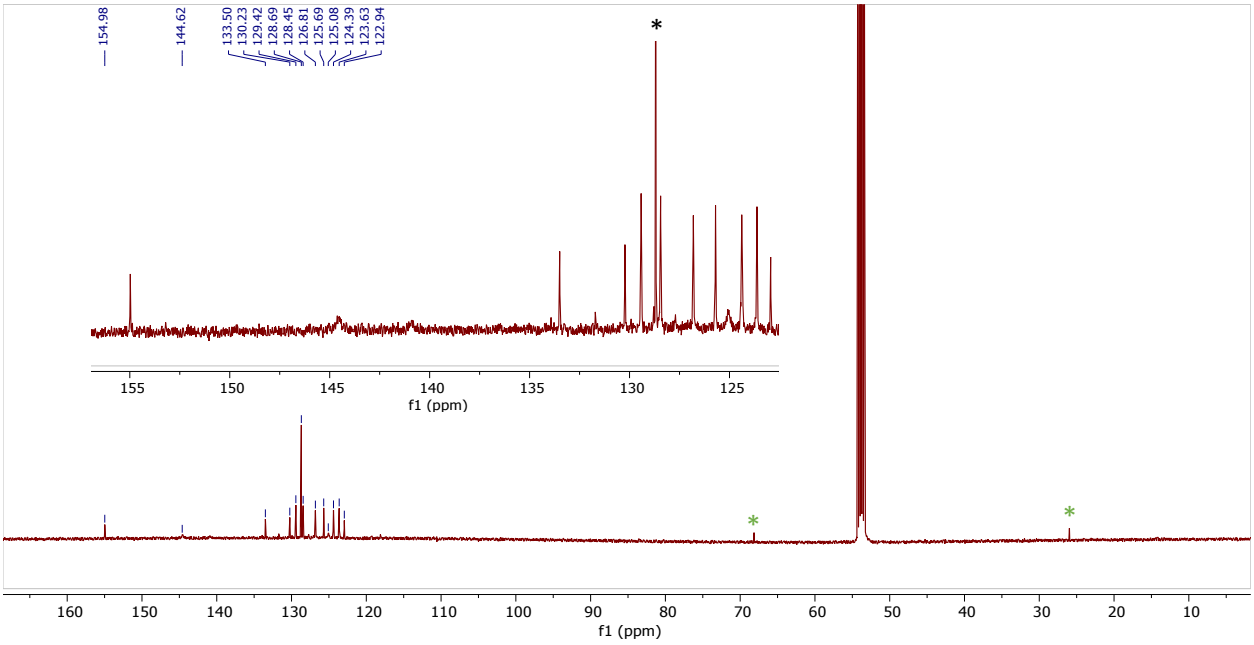

Figure S37. $^{13}C\{H\}$ NMR spectrum of (*R*)-**8** in CD_2Cl_2 (* THF; * C_6H_6).

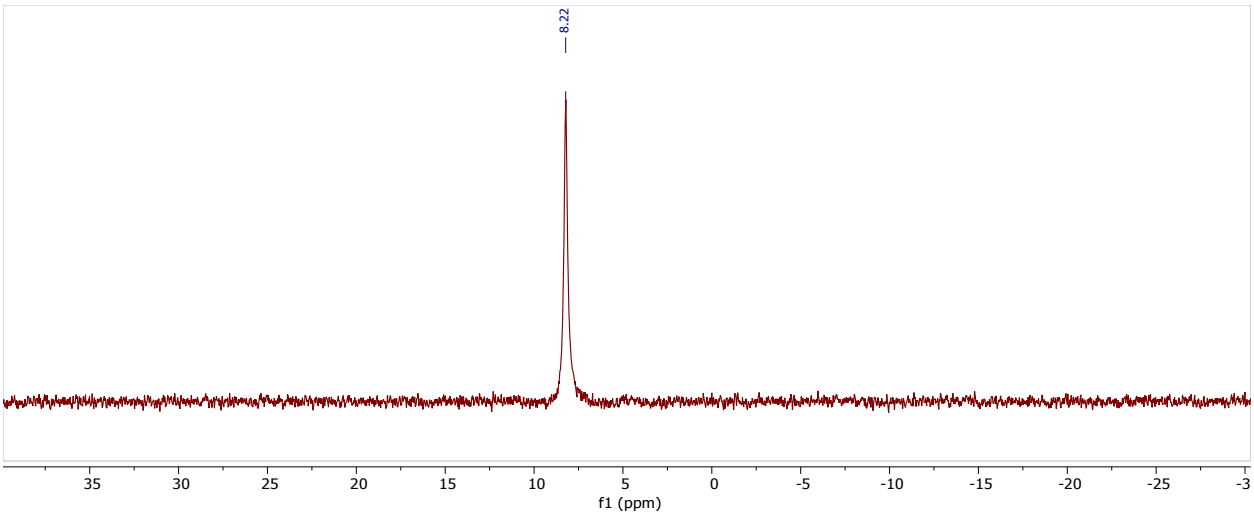

Figure S38. $^{11}B\{H\}$ NMR spectrum of (*R*)-**8** in CD_2Cl_2.

Formation of (*R*)-**8** in THF

In the glove box, a J-Young NMR tube was charged with (*R,R,R*)-**5** (20 mg, 0.023 mmol), anhydrous pyridine (4 mg, 0.05 mmol) and 0.5 mL of THF. The progress of the reaction was monitored by ^{11}B NMR spectroscopy (see below).

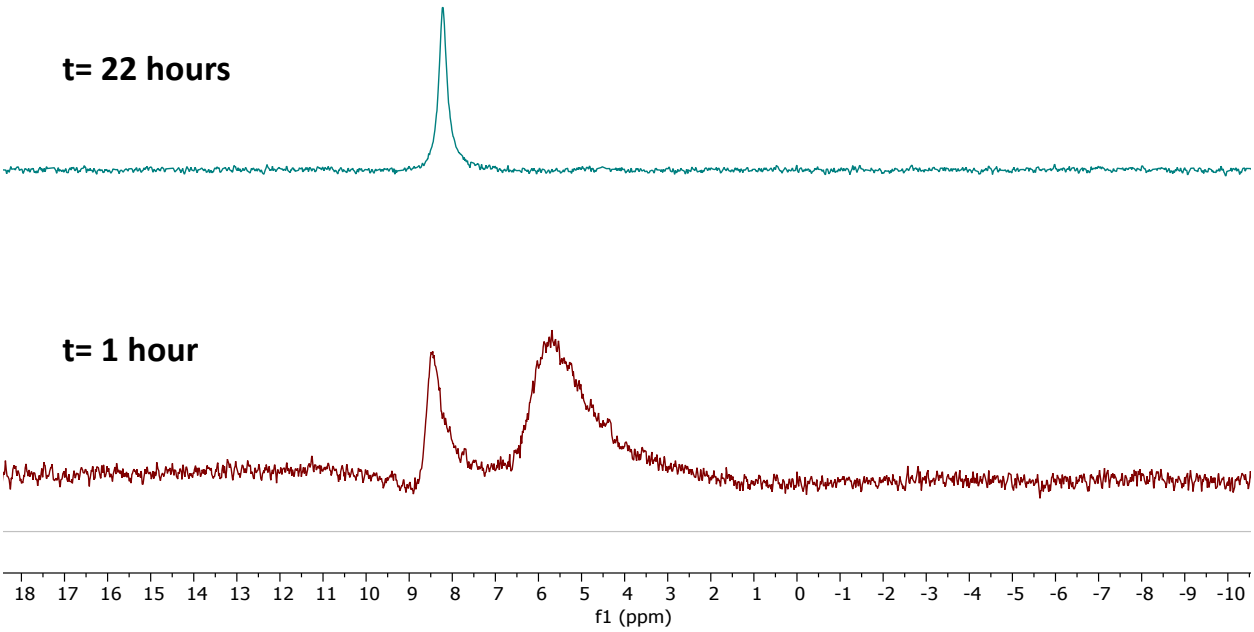

Figure S39. Stack plot of $^{11}B\{H\}$ NMR spectra of the reaction of (*R,R,R*)-**5** with pyridine in THF at room temperature.

2.10. Synthesis of (*R*)-**9**

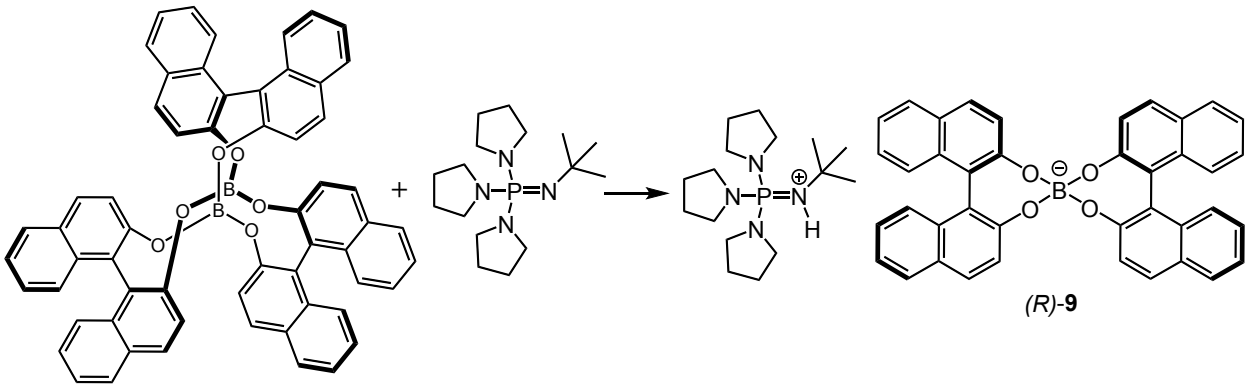

Under nitrogen, a 50 ml Schlenk flask equipped with a magnetic stir bar was charged with (*R,R,R*)-**5** (50 mg, 0.057 mmol) and dry THF (10 mL). To this clear solution, a solution of $(pyrr)_3P{=}NBu^t$ (17.9 mg, 0.057 mmol) in THF (5 mL) was added and left at room temperature. The obtained product subsequently precipitated and was washed thrice with THF and dried under vacuum to give 30 mg of (*R*)-**9** [59% based on (*R,R,R*)-**5**]. ^{1}H NMR (CD_2Cl_2, 400 MHz): 0.7 (br, CH_3, 9 H), 1.32-1.46 (br, CH_2, 12 H), 2.65-2.79 (br, NCH_2, 12 H), 3.40 (d, $^1J_{P\text{-}H}$ = 10.7 Hz, 1 H), 7.10-7.14 (m, CH arom., 4 H), 7.25-7.29 (m, CH arom., 8 H), 7.44 (d, $^3J_{H\text{-}H}$ = 8.68 Hz, CH arom., 4 H), 7.89 (t, $^3J_{H\text{-}H}$ = 8.4 Hz, CH arom., 8 H) ppm. ^{13}C{H} NMR (CD_2Cl_2,125.79 MHz): δ 26.1, 31.0, 47.6, 122.7, 122.9, 124.9, 125.3, 127.0, 128.3, 128.6, 130.0, 133.8, 156.8 ppm. ^{11}B NMR (CD_2Cl_2 (128.4 MHz): δ 8.2 ppm. ^{31}P NMR (CD_2Cl_2, 161.9 MHz): δ 21.8 ppm. IR (solid) $\tilde{\nu}_{(N\text{-}H)}$ = 3267 cm^{-1} (broad). Calc. for $C_{56}H_{59}BN_4O_4P$ (892.90): C, 75.33; H, 6.55; Found C, 74.60; H, 6.66.

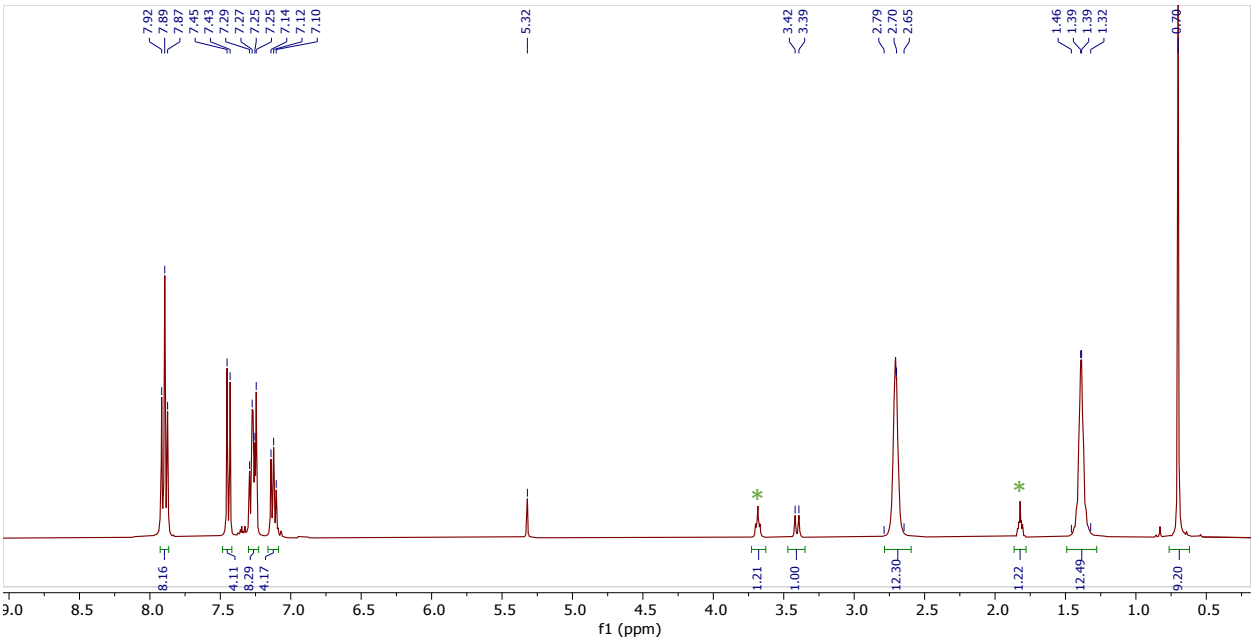

Figure S40. ^{1}H NMR spectrum of (*R*)-**9** in CD_2Cl_2 (* THF).

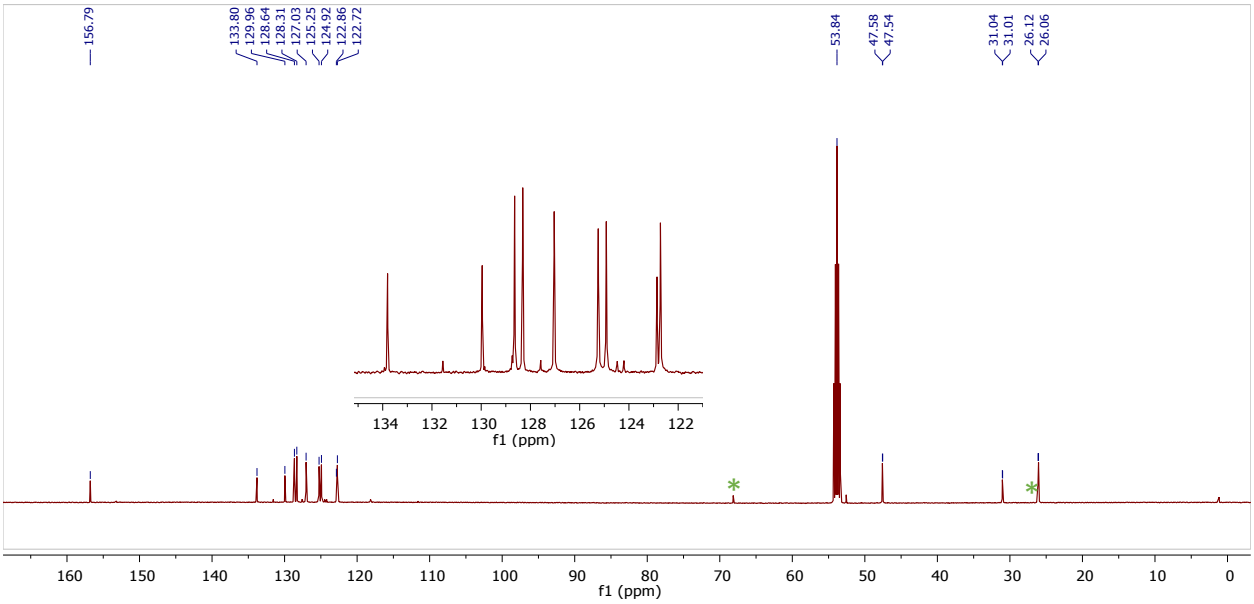

Figure S41. ^{13}C{H} NMR spectrum of (*R*)-**9** in CD_2Cl_2 (* THF).

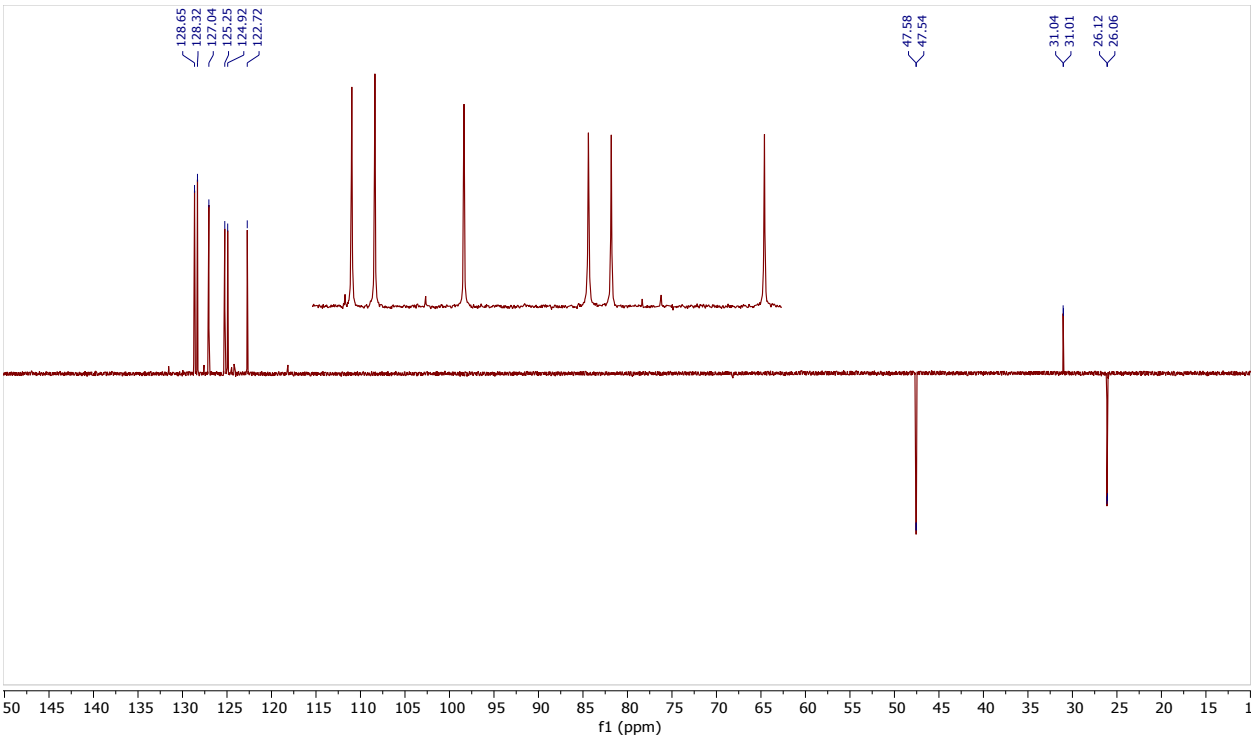

Figure S42. $^{13}C\{H\}$ (DEPT-135) NMR spectrum of (*R*)-**9** in CD_2Cl_2.

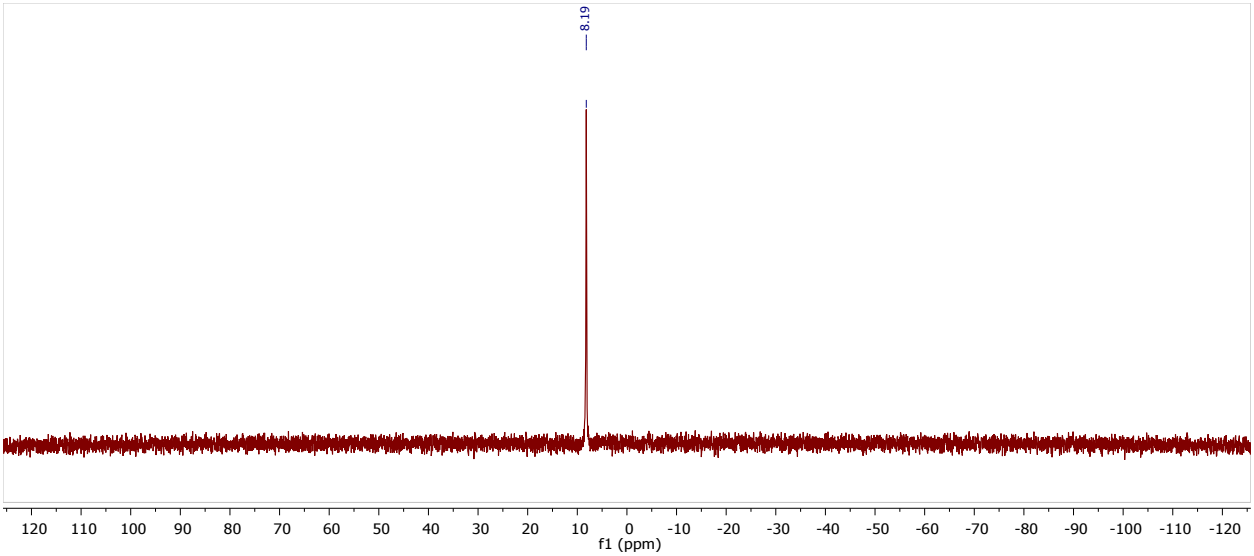

Figure S43. $^{11}B\{H\}$ NMR spectrum of (*R*)-**9** in CD_2Cl_2.

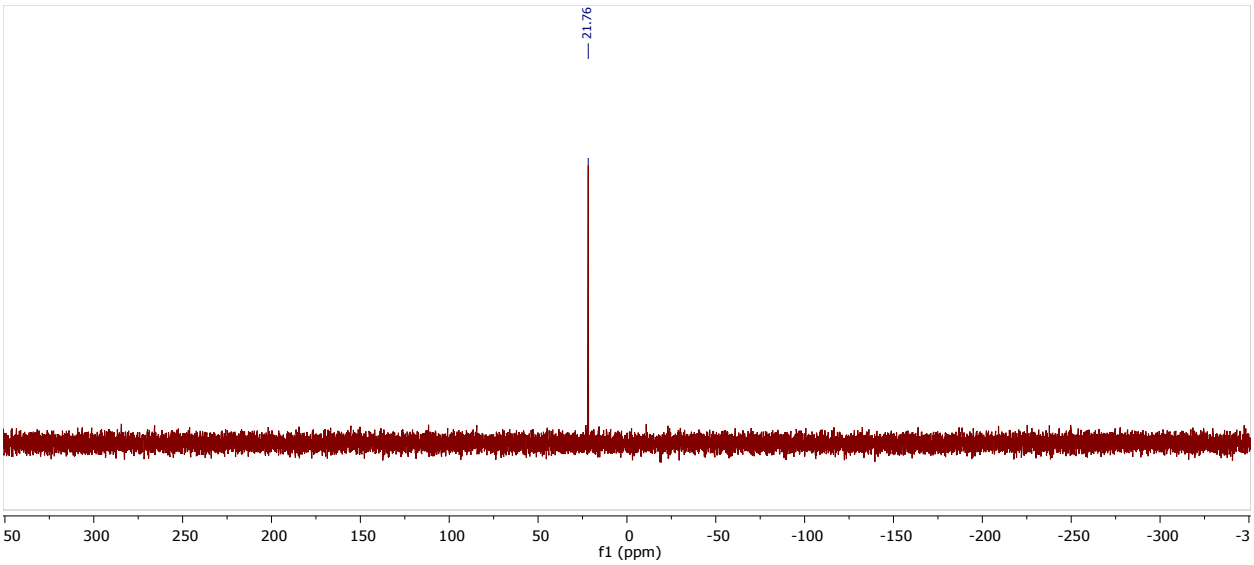

Figure S44. $^{31}P\{H\}$ NMR spectrum of (*R*)-**9** in CD_2Cl_2.

Formation of (*R*)-**9** in C_6D_6

In the glove box, a J-Young NMR tube was charged with (*R,R,R*)-**5** (20 mg, 0.023 mmol), $(pyrr)_3P{=}NBu^t$ (7.4 mg, 0.023 mmol) and 0.5 mL of C_6D_6. The obtained precipitate was washed with C_6D_6, dried under vacuum and analyzed by NMR spectroscopy.

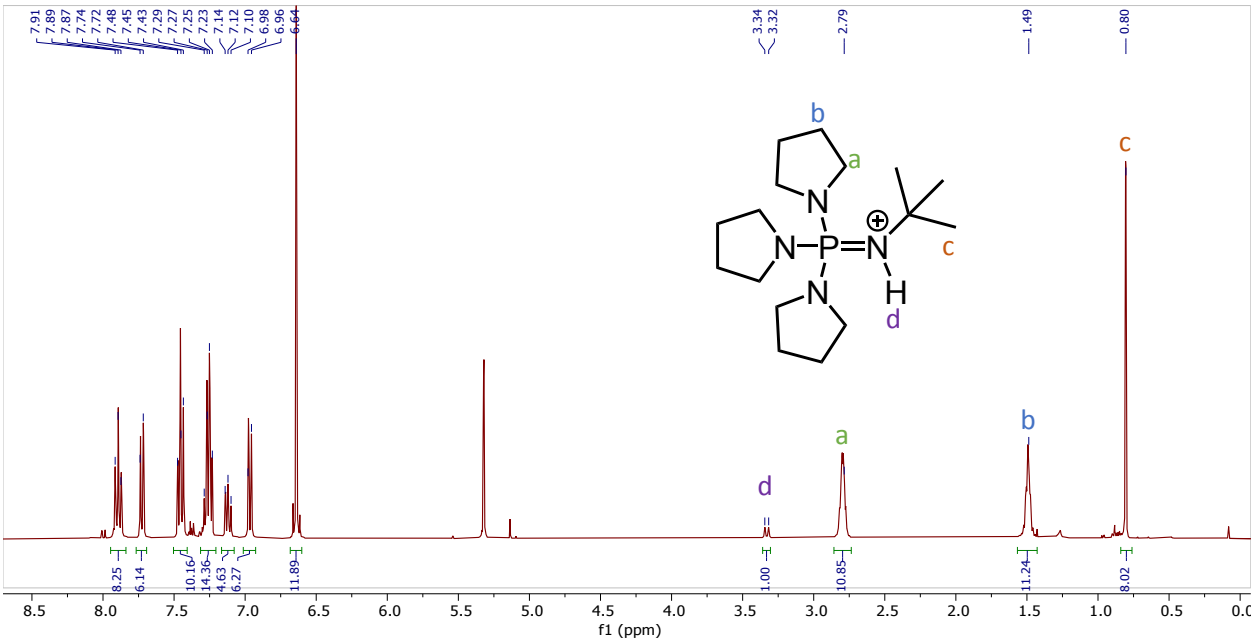

Figure S45. ^1H NMR spectrum of (*R*)-**9** in CD_2Cl_2 (contains unidentified impurities).

2.11. Reactions of (*R,R,R*)-**5** with 1,3-bis(2,4,6-trimethylphenyl)-1,3-dihydro-2H-imidazol-2-ylidene

In the glove box, a 50 ml Schlenk flask equipped with a magnetic stir bar was charged with (*R,R,R*)-**5** (25 mg, 0.03 mmol) and 10 mL of dry benzene. To this clear solution, 1,3-bis(2,4,6-trimethylphenyl)-1,3-dihydro-2H-imidazol-2-ylidene (9 mg, 0.03 mmol) in dissolved in benzene (5 mL) was added and left at room temperature. After two days, a few crystals of (*R*)-**10** were formed. Attempts to isolate and fully characterize (*R*)-**10** failed due its thermal instability and moisture sensitivity.

3. Catalytic Experiments

3.1 General procedure

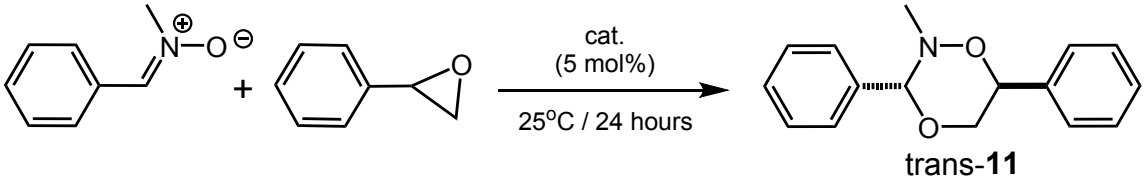

trans-**11**

In the glove box, a 4 mL scintillation vial with septum screw cap equipped with a magnetic stir bar was charged with PhCH=N(O)Me (0.17 mmol), catalyst (0.008 mmol) and 0.5 mL toluene. After styrene oxide (0.17 mmol) was added to this solution, the mixture was stirred at room temperature for 24 hours. Then an aliquot was taken from the reaction mixture and added to an NMR tube. $CDCl_3$ was added to the NMR tube and the resulting clear solution was analyzed by ^1H NMR spectroscopy. After complete conversion, the reaction mixture was passed over silica gel column (pipette) to give ca. 85% of pure trans-**11**. The analytical data are in agreement with those reported in the literature [4]. The enantiomeric ratio was determined by HPLC. (Column used: Chiral AD, 0.5 mL/min, 10% *i*-PrOH/hexane).

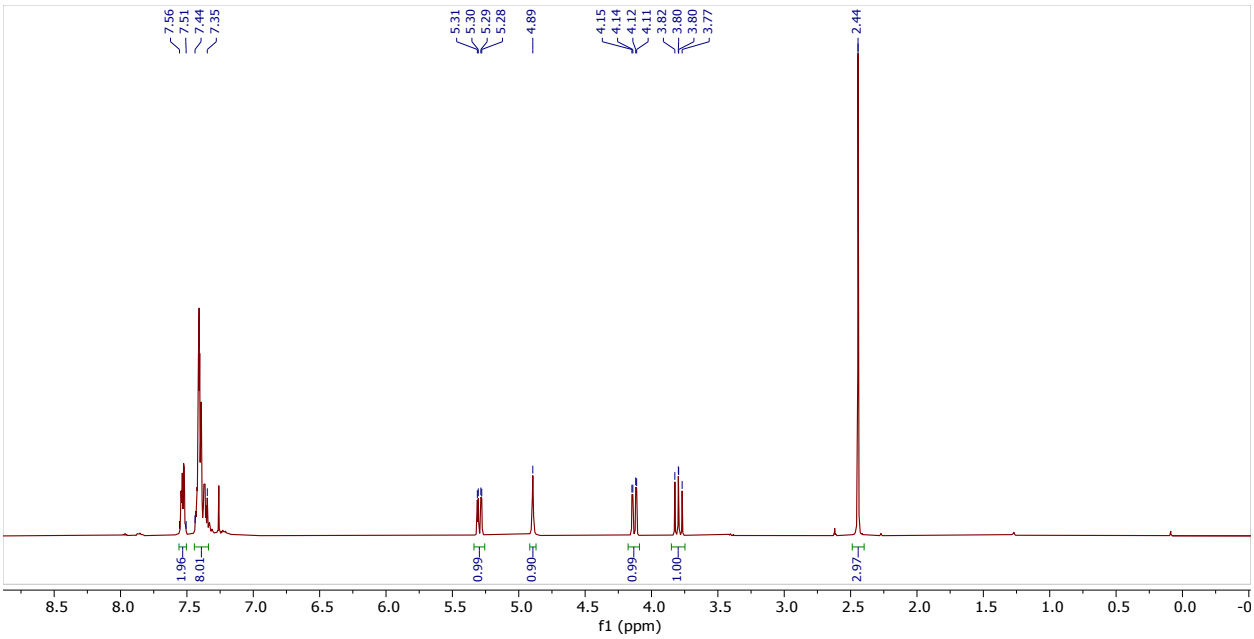

Figure S46. ^{1}H NMR spectrum of trans-**11** in $CDCl_3$.

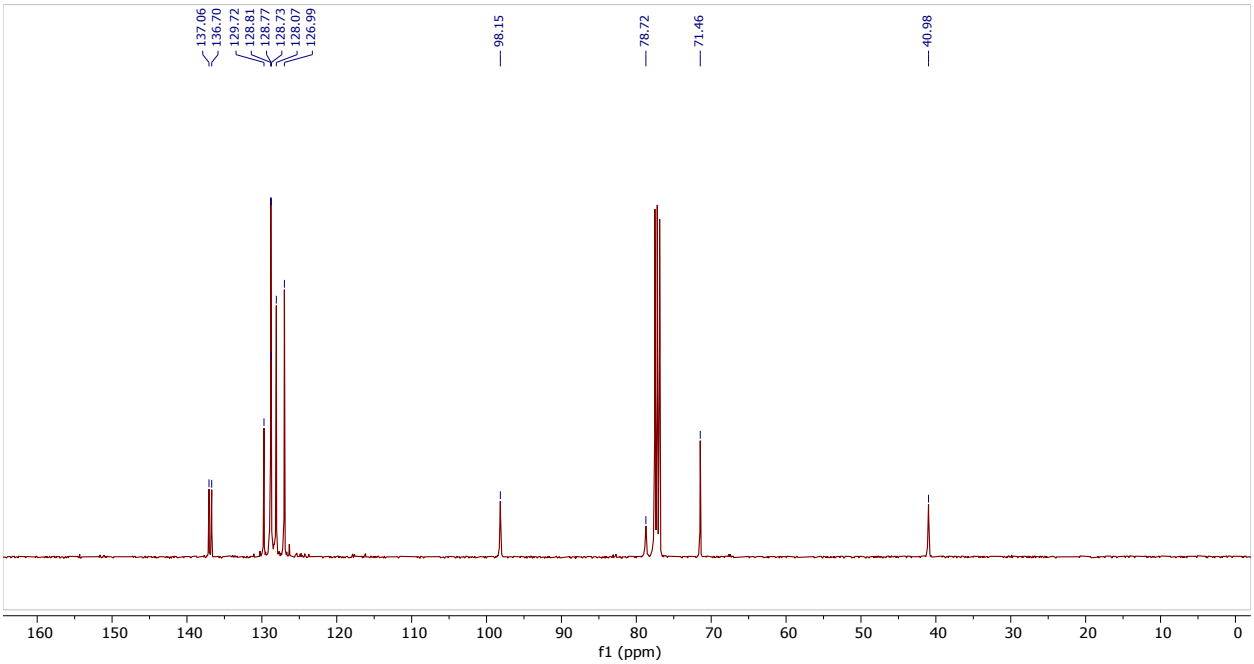

Figure S47. $^{13}C\{H\}$ NMR spectrum of trans-**11** in $CDCl_3$.

3.2 General procedure for kinetic studies

In the glove box, a J-Young NMR tube was charged with catalyst (0.0075 mmol), PhCH=N(O)Me (20 mg, 0.15 mmol), *rac*-styrene oxide (18 mg, 0.15 mmol), 1,3,5-trimethoxybenzene (25 mg, 0.15 mmol) as internal standard and 0.5 mL of C_6D_6 and reaction mixture was analyzed by ^1H NMR spectroscopy.

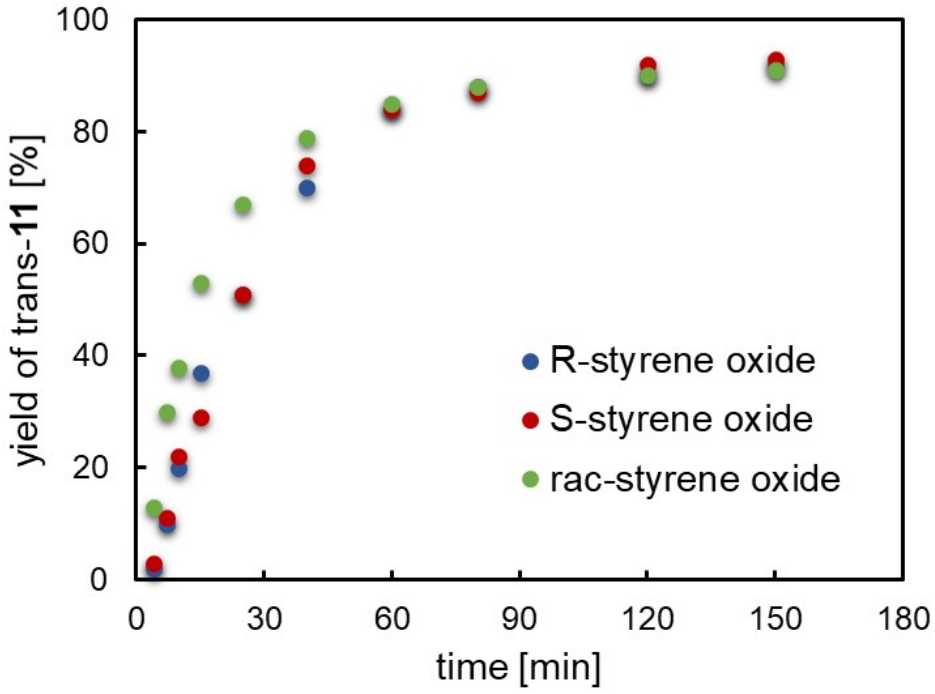

Figure S48. Evolution of yield in the Lewis acid catalyzed annulation of (R)-, (S)- and *rac*-styrene oxide with PhCH=NMe(O) to trans-**11** with 5 mol% of (*R*)-**1** as the catalyst.

3.2 Kinetic resolution experiment

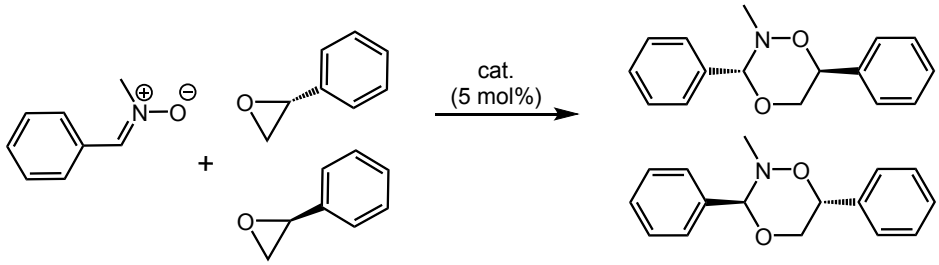

trans-**11**

In the glove box, a J-Young NMR tube was charged with (*R*)-**1** (4.4 mg, 0.008 mmol), PhCH=N(O)Me (22 mg, 0.16 mmol), *rac*-styrene oxide (40 mg, 0.33 mmol) and 0.5 mL of C_6D_6. After two hours, 94% of trans-**11** was formed as determined by ^{1}H NMR spectroscopy. The reaction mixture was then passed over silica gel column (pipette) to give pure trans-**11**. The enantiomeric excess was found to be 9% as determined by HPLC.

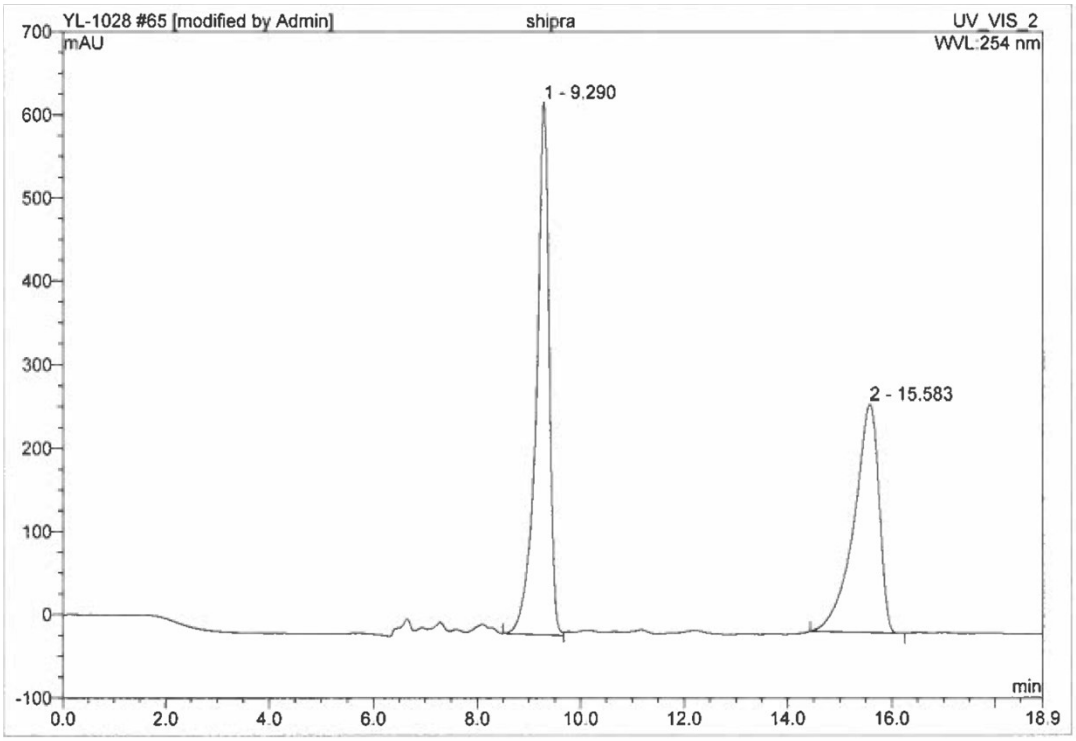

No.	Ret.Time min	Peak Name	Height mAU	Area mAU*min	Rel.Area %	Amount	Type
1	9.29	n.a.	639.511	182.486	54.43	n.a.	BM *
2	15.58	n.a.	274.604	152.794	45.57	n.a.	BMB*
Total:			914.115	335.280	100.00	0.000	

4. Stoichiometric Experiments

4.1. Reaction of (*R*)-**1** with trans-**11**

In the glove box, a J-Young NMR tube was charged with (*R*)-**1** (50 mg, 0.094 mmol), trans-**11** (24 mg, 0.094 mmol) and 0.5 mL of C_6D_6. Analysis of the mixture by ^1H NMR spectroscopy revealed no reaction between (*R*)-**1** and trans-**11**.

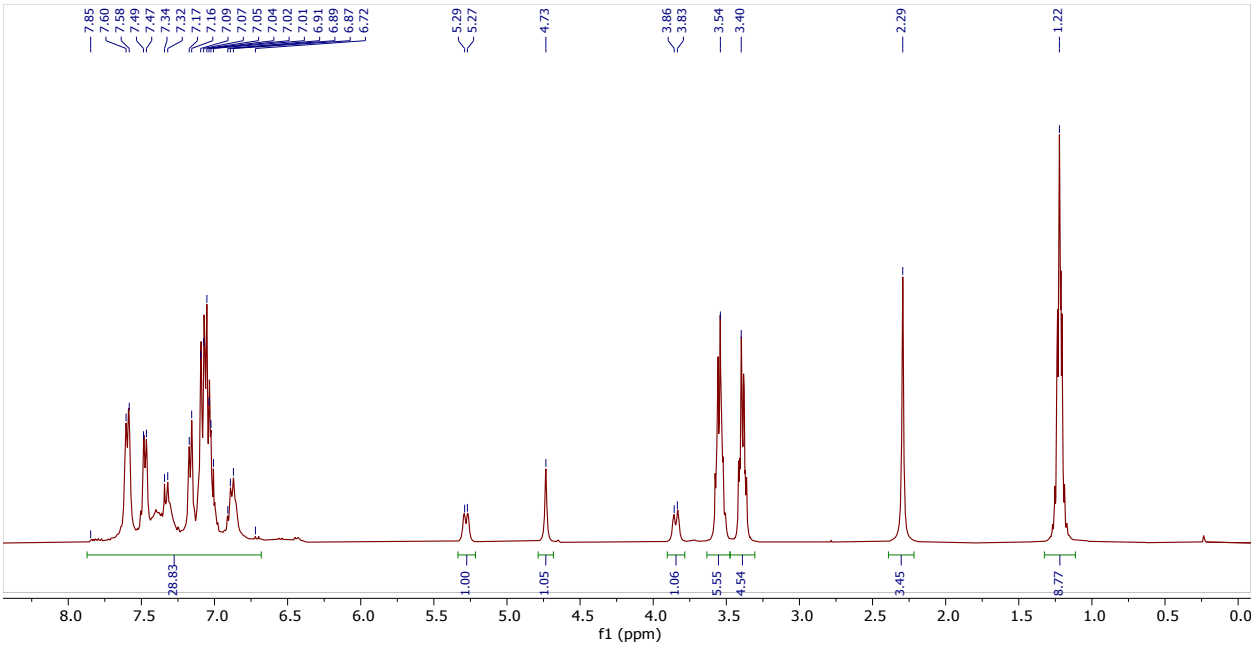

Figure S49. ^1H NMR spectrum in C_6D_6.

4.2. Reaction of (*R,R*)-**2** with trans-**11**

In the glove box, a J-Young NMR tube was charged with (*R,R*)-**2** (50 mg, 0.054 mmol), trans-**11** (28 mg, 0.11 mmol) and 0.5 mL of C_6D_6. Analysis of the mixture by ^1H NMR spectroscopy revealed no reaction between (*R,R*)-**2** and trans-**11**.

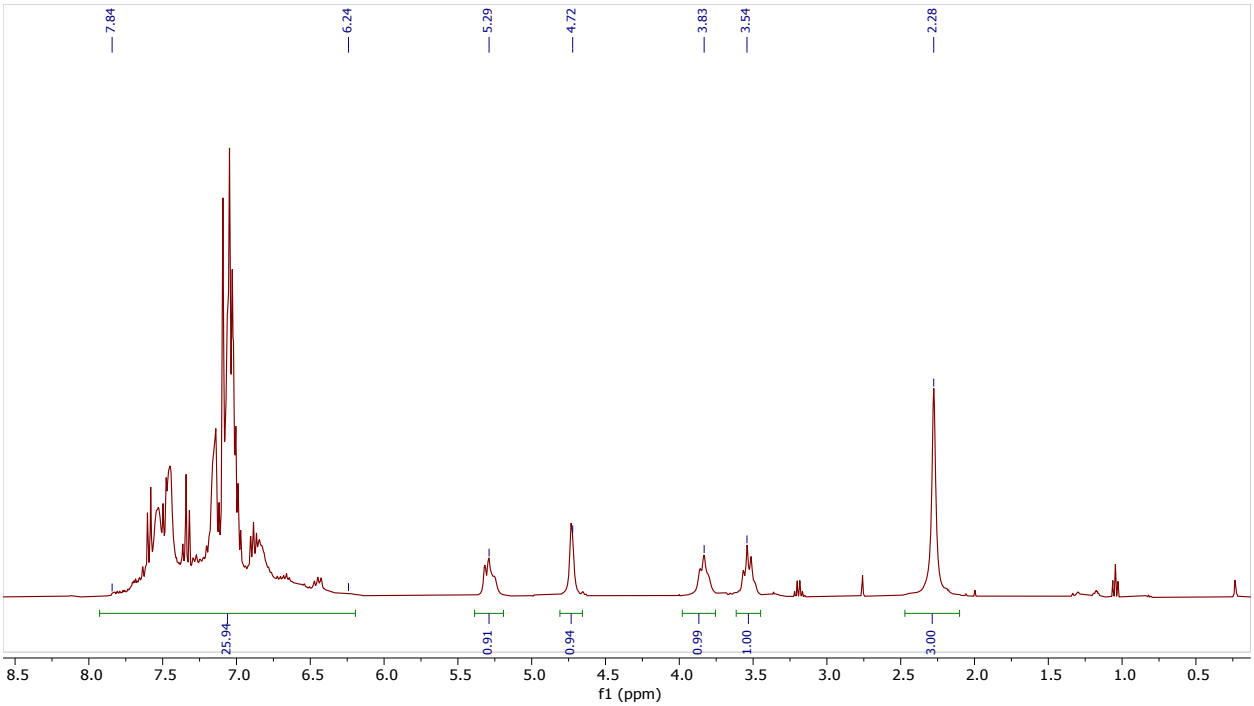

Figure S50. ^1H NMR spectrum in C_6D_6.

4.3. Reaction of (*R*)-**1** with PhCH=N(O)Me and (*R*)-styrene oxide

In the glove box, a J-Young NMR tube was charged with (*R*)-**1** (68 mg, 0.13 mmol), PhCH=N(O)Me (17 mg, 0.13 mmol), (*R*)-styrene oxide (30 mg, 0.25 mmol) and 0.5 mL of C_6D_6. Analysis of the mixture by ^{1}H NMR spectroscopy revealed formation of trans-**11** along with small quantities of oligo/polymerized styrene oxide.

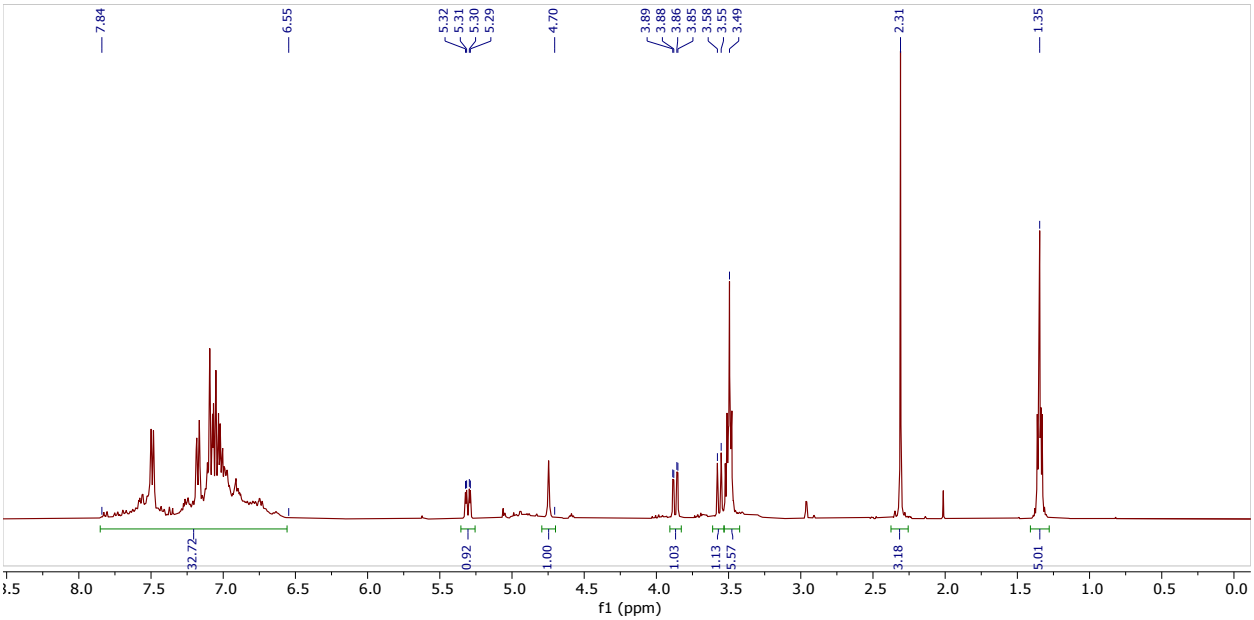

Figure S51. ^{1}H NMR spectrum in C_6D_6.

4.4. Reaction of (*R,R*)-**2** with PhCH=N(O)Me and *rac*-styrene oxide

In the glove box, a J-Young NMR tube was charged with (*R,R*)-**2** (32 mg, 0.035 mmol), PhCH=N(O)Me (9.5 mg, 0.07 mmol), *rac*-styrene oxide (20 mg, 0.17 mmol) and 0.5 mL of C_6D_6. Analysis of the mixture by ^{1}H NMR spectroscopy revealed formation of trans-**11** along with small quantities of oligo/polymerized stryrene oxide.

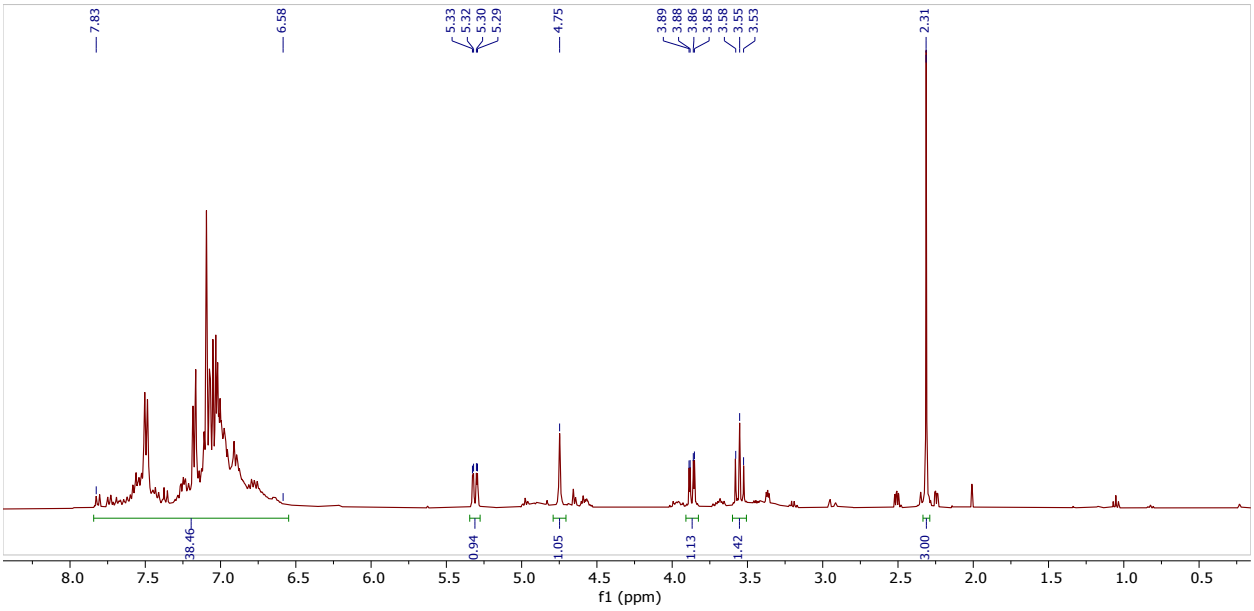

Figure S52. ^{1}H NMR spectrum in C_6D_6.

5. X-ray Crystallography

CCDC2058920 (*R*)-**1**, CCDC2058921 (*R,R*)-**2**, CCDC2058922 (*R*)-**3**, CCDC2058923 (*R*)-**10**, CCDC2058924 (*R,S*)-**2**, CCDC2058925 (*R*)-**9** and CCDC2068872 (*R*)-**8** contain the supplementary crystallographic data for this paper.

These data can be obtained from the Cambridge Crystallographic Data Centre via http://www.ccdc.cam.ac.uk/data_request/cif, or from the Cambridge Crystallographic Data Centre, 12 Union Road, Cambridge CB2 1EZ, UK; fax: (+44) 1223-336-033; e-mail: deposit@ccdc.cam.ac.uk.

General Data Collection

Data for structures *(R,R)*-**2**, *(R)*-**3** and *(R)*-**10** were collected on a Bruker PLATFORM three-circle diffractometer equipped with an APEX II CCD detector. The instrument was operated at 1500 W (50kV, 30 mA) to generate (graphite monochromated) Mo Kα radiation (λ = 0.71073 Å). Data for structures *(R)*-**1**, *(R,S)*-**2**, *(R)*-**8** and *(R)*-**9** were collected on a Rigaku XtaLAB Synergy-*i* Kappa diffractometer equipped with a PhotonJet-*i* X-ray source operated at 50 W (50kV, 1 mA) to generate Cu Kα radiation (λ = 1.54178 Å) and a HyPix-6000HE HPC detector. All crystals were transferred from their respective vials and placed on glass slides in NVH Cargille immersion oil. A Zeiss Stemi 305 microscope was used to identify a suitable specimen for each X-ray diffraction experiment from a representative sample of the material. The crystal and a small amount of the oil were collected on a MiTeGen cryoloop and transferred to the instrument where it was placed under a cold nitrogen stream (Oxford 700) maintained at 100K throughout the duration of the experiment. The samples were optically centered individually with the aid of a video camera to insure that no translations were observed as the crystals were rotated through all positions. A unit cell collection was then carried out on each sample. After it was determined that the unit cell was not present in the CCDC database, a data set was collected. After data collection, the crystals were measured for size, morphology, and color, information of which can be found in the corresponding CIF for each structure.

Refinement Details

After data collection, the unit cell was re-determined using a subset of the full data collection. Intensity data for structures *(R,R)*-**2**, *(R)*-**3**, and *(R)*-**10** were corrected for Lorentz, polarization, and background effects using SAINT [5]. A semi-empirical correction for adsorption was applied to these structures using the program *SADABS* [6]. For structures *(R,S)*-**2**, *(R)*-**9**, *(R)*-**8** and *(R)*-**1** intensity data were corrected for Lorentz, polarization, and background effects using *CrysAlis*^{Pro} [7]. A numerical absorption correction was applied based on a Gaussian integration over a multifaceted crystal and followed by a semi-empirical correction for adsorption applied using the program *SCALE3 ABSPACK* [8]. The programs *SHELXT* [9] was used for structure solution and *SHELXT* [10] was used for structure refinement of the crystal structures within the OLEX2 software [11]. For all structures, hydrogen atoms bound to carbon atoms were located in the difference Fourier map and were geometrically constrained using the appropriate AFIX commands, unless otherwise noted. Unique structure refinement details are listed below for the following structures.

(R)-**1**

The interstitial tetrahydrofuran molecule was positionally disordered and atoms O4 and C31 < C34 were split into two sites A and B. The site occupancies of the A and B site refined to 0.84 and 0.16, respectively. To help maintain reasonable ADP values and bond lengths, SIMU, RIGU and free variable DFIX restraints were applied to the disordered sites.

(R,R)-**2**

After data collection, the unit cell was re-determined using a subset of the full data collection. At this point it was determined that crystal was composed of two components that were treated with *CELL_NOW* [12]. After corrects for Lorentz, polarization, and background effects a semi-empirical correction for adsorption was applied using the program *TWINABS* [13]. Phenyl rings containing carbon atoms C1 < C6, C53 < C58, and C99 < C104 were also constrained with the AFIX 66 command to maintain reasonable C-C bond lengths. Ultimately, the structure was refined against HKLF5 file containing only

reflections from the primary domain with a final BASF parameter was 0.404. Also, the Z' value for this structure is 2.

(R)-**3**

Within the structure, there was positional disorder about two of the interstitial benzene molecules. The carbon atoms C94 < C99 sites were split into parts A and B, while the benzene ring containing atoms C100 < C106 and C107 < C111 were allowed to free refine their site occupancies to a total value of 1. The site occupancy values were 0.62 and 0.38 for parts A and B and 0.47 and 0.53 for rings starting with C100 and C107, respectively. To help model the minor components, the AFIX 66 constraint was applied to the disordered rings. To help maintain reasonable ADP values, the SIMU and RIGU restraints were applied to the disordered sites as well. After all the atoms positions were refined, the TWIN lab -1 0 0 0 -1 0 0 0 -1 was suggested and applied with a final BASF value of 0.358.

(R,S)-**2**

After all of the major atoms were determined, it was determined that the interstitial space within the structure contained highly disordered diethyl ether molecules from crystallization. This electron density was account for by applying the use of a solvent mask in the OLEX2 software [11] and account for 62.5 eV in the unit cell (~1.5 diethyl ether molecules).

(R)-**8**

After data collection, the unit cell was re-determined using a subset of the full data collection. Intensity data were corrected for Lorentz, polarization, and background effects using the *CrysAlis*^{Pro} [7]. A spherical absorption correction was applied based on a Gaussian integration and followed by a semi-empirical correction for adsorption applied using the program *SCALE3 ABSPACK* [8]. The *SHELX-2018* [9, 10], series of programs was used for the solution and refinement of the crystal structure within OLEX2 software [11]. The structure was initially solved in the space group *P*1 and after the final refinements, the software Platon [14] was used to confirm the space group. Within the structure, there were six crystallographically unique tetrahydrofuran molecules, of which four of them were positionally disordered to different extents. To help maintain reasonable ADP and bond distance values, SIMU, RIGU, and free variable DFIX restraints were

applied to the disordered sites. Hydrogen atoms bound to carbon and nitrogen atoms were geometrically constrained using the appropriate AFIX commands. The Z' value for the structure is 2.

(R)-**9**

The dichloromethane molecules in the interstitial space of structure were positionally disordered over multiple sites. To maintain reasonable ADP and bond lengths for these disordered molecules, SIMU and free variable DFIX restraints were applied where needed. The majority of the hydrogen atoms bound to carbon and nitrogen atoms were geometrically constrained using the appropriate AFIX commands. The hydrogen atom bound to N1 (H1) was allowed to refine its position.

6. References

[1] Fuller, A.; Hughes, D.; Lancaster, S.; White, C. *Organometallics* **2010**, *29*, 2194-2197.

[2] Yavuz, S.; Ozkan, H.; Colak, N.; Yildirir, Y. *Molecules* **2011**,*16*, 6677.

[3] Thormeier, S.; Carboni, B.; Kaufmann, D. *J. Organomet. Chem.* **2002**, *657*,136-145.

[4] Pathipati, S. R.; Singh, V.; Eriksson, L.; Selander, N. *Org. Lett.* **2015**, *17*, 4506-4509.

[5] Bruker SAINT and Apex3 v 2017.3-0, **2017**.

[6] Krause *et al.*, SADABS v 2016/2, **2015**.

[7] CrysAlis^{Pro} Oxford Diffraction Ltd., **2018**.

[8] SCALE3 ABSPACK Oxford Diffraction Ltd. **2005**.

[9] Sheldrick, G. M., *Acta Crystallogr*. **2015**, *A**71***, 3-8.

[10] Sheldrick, G. M., *Acta Crystallogr*. **2015**, *C**71***, 3-8.

[11] Dolomanov, O. V.; Bourhis, L. J.; Gildea, R. J.; Howard, J. A. K.; Puschmann. H., *J. Appl. Cryst*. **2009**, *42*, 339-341.

[12] Sheldrick, G. M., *Acta Crystallogr.* **2008**, *A64*, 112-122.

[13] Sheldrick, G. M., TWINABS 2012/1. Bruker, Madison, Wisconsin, USA, **2012**.

[14] Spek, A. L., *J. Appl. Cryst.* **2003**, *36*, 7-11.